Gödelian Index Theorem for Chaotic Systems (Part 3): Extending Atiyah-Singer with Gödelian Ricci Flow and Application to Hyperion's Chaotic Orbit

Paul Chun-Kit Lee, MD
Division of Cardiology, New York University, New York

09/02/24

Abstract

This paper introduces the Gödelian-Logical Flow (GLF) framework, which bridges Gödel's incompleteness theorems with classical chaos theory. The framework defines two key functions for chaotic systems: the truth function (Φ) and the provability function (P), inspired by formal logic. These functions are used to define the Gödelian Unpredictability Index (GUI), which quantifies logical unpredictability. Additionally, we introduce a modified Ricci flow—termed Gödelian Ricci Flow—which governs the evolution of both the geometric structure of a system and its logical attributes.

We apply the GLF framework to four classical chaotic systems: the Lorenz system, double pendulum, fluid dynamics, and Hyperion's chaotic rotation. For each system, we derive specific formulations for the Φ and P functions, relating them to physical quantities such as kinetic energy and angular momentum. The GUI is computed for these systems, offering complementary information to established chaos measures, such as Lyapunov exponents. Our results suggest that the GUI identifies regions of high logical complexity in phase space, providing insights into chaotic dynamics from a logical perspective.

In the case of Hyperion's chaotic rotation, we demonstrate how the GUI correlates with the moon's kinetic energy and angular velocity, highlighting regions where logical unpredictability is most pronounced. This novel approach provides a fresh lens to analyze chaotic systems by integrating formal logic with classical dynamical measures.

Though primarily theoretical, the GLF framework opens the possibility of exploring how logical complexity interacts with chaotic dynamics, extending beyond traditional geometric or physical analysis. By incorporating logical structures into the study of chaotic systems, this framework offers potential avenues for future research into the relationship between logic, geometry, and unpredictability in complex systems.

Contents

1 Executive Summary

In the realms of mathematics and physics, Gödel's incompleteness theorems and chaos theory have long been subjects of intense study. This paper introduces the Gödelian-Logical Flow (GLF) framework, a novel approach that bridges these two domains, offering new insights into the nature of unpredictability in chaotic systems.

The GLF framework introduces two key functions: the truth function $\Phi(x)$ and the provability function $P(x)$. These functions, inspired by concepts from formal logic, are applied to the state space of chaotic systems. Their interplay gives rise to the Gödelian Unpredictability Index (GUI):

$$GUI(x) = |\Phi(x) - P(x)|$$

This index quantifies a new aspect of chaotic behavior that complements traditional measures like Lyapunov exponents.

For mathematicians and physicists, we present the formal definition of a Gödelian-Topos Manifold (M, g, Φ, P) and the Gödelian Ricci Flow equations:

$$\frac{\partial g}{\partial t} = -2Ric(g) - \nabla\Phi \otimes \nabla\Phi - \nabla P \otimes \nabla P$$

$$\frac{\partial \Phi}{\partial t} = \Delta_g \Phi + |\nabla \Phi|^2$$

$$\frac{\partial P}{\partial t} = \Delta_g P + (\Phi - P)$$

These equations describe the evolution of the system's geometry and logical structure over time.

We apply the GLF framework to four classical chaotic systems:

- **The Lorenz system,** where we define:

  $$\Phi(x, y, z) = 1 - \exp(-k_1(x^2 + y^2 + z^2)), \quad P(x, y, z) = 1 - \exp(-k_2|\nabla \cdot f(x, y, z)|)$$

- **The double pendulum**
- **Fluid dynamics**
- **Hyperion's chaotic rotation**

In each case, we demonstrate how the GLF approach can offer new insights into the behavior of these systems, potentially revealing aspects of their dynamics not captured by traditional chaos theory alone.

A key finding is that the GUI often identifies regions of high unpredictability that don't always align with those highlighted by Lyapunov exponents. This suggests that logical unpredictability, as captured by GUI, represents a distinct aspect of chaotic behavior.

The paper also presents the Gödelian Index Theorem:

$$ind_G(D) = \int_M \hat{A}_G(M)\, ch_G(\sigma(D))\, Todd_G(TM \otimes \mathbb{C})$$

This theorem provides a rigorous mathematical foundation for our approach, connecting it to established concepts in differential geometry.

To validate our theoretical framework, we conducted extensive numerical simulations. The results, detailed in the appendices, support the utility of the GLF approach in providing new perspectives on chaotic dynamics.

This work opens up new avenues for understanding unpredictability in complex systems, offering a fresh perspective at the intersection of mathematical logic and chaos theory. While the focus of this paper is on theoretical foundations and applications in classical chaotic systems, the framework's potential extends to various fields where complex, unpredictable behavior is observed.

2 Introduction and Motivation

The Gödelian-Logical Flow (GLF) framework introduced in this paper attempts to bridge concepts from Gödel's incompleteness theorems [9] with chaos theory. By applying concepts inspired by Gödel's work to the study of chaotic systems, we aim to shed new light on the nature of unpredictability in complex physical phenomena [15, 16].

The GLF framework introduces two key functions: a "truth" function (Φ) and a "provability" function (P). These functions, inspired by concepts from formal logic, are applied to the state space of chaotic systems. The interplay between these functions gives rise to a measure we call the Gödelian Unpredictability Index (GUI), which quantifies a new aspect of chaotic behavior that complements traditional measures like Lyapunov exponents.

Our work explores how this framework can be applied to various classical chaotic systems, including the Lorenz system, the double pendulum, fluid dynamics, and even the chaotic rotation of Saturn's moon Hyperion. Through these applications, we demonstrate how the GLF approach can offer new insights into the behavior of these systems, potentially revealing aspects of their dynamics that are not captured by traditional chaos theory alone.

2.1 Key Concepts and Results

Our work introduces several novel mathematical constructs that form the backbone of our theoretical framework. These include:

- **Gödelian-Topos Manifolds (Definition 1.1):** We define a Gödelian-Topos Manifold as a tuple (M, g, Φ, P) where M is a smooth n-dimensional manifold, g is a Riemannian metric, and $\Phi, P : M \to [0, 1]$ are smooth functions satisfying $P \leq \Phi$ pointwise. This structure allows us to incorporate logical concepts into the geometric framework of differential manifolds [17, 19].

- **Gödelian Ricci Flow (Definition 2.1):** Building on the classical Ricci flow, we introduce a modified flow that incorporates our Gödelian functions [17]:

$$\frac{\partial g}{\partial t} = -2\, Ric_G, \quad \frac{\partial \Phi}{\partial t} = \Delta_g \Phi + |\nabla \Phi|_g^2, \quad \frac{\partial P}{\partial t} = \Delta_g P + (\Phi - P)$$

  This flow provides a dynamic perspective on how the geometry of our manifold evolves in tandem with the logical structures we've imposed.

- **Discrete Gödelian Ricci Flow (Definition 5.1):** For a time-dependent Gödelian graph $G(t) = (V, E(t), \Phi(t), P(t))$, we define:

$$\frac{d}{dt}w_{ij}(t) = -2Ric_{ij}(t) - \nabla_i\Phi(t)\nabla_j\Phi(t) - \nabla_i P(t)\nabla_j P(t)$$

$$\frac{d}{dt}\Phi_i(t) = \Delta_G\Phi_i(t) + |\nabla\Phi_i(t)|^2$$

$$\frac{d}{dt}P_i(t) = \Delta_G P_i(t) + (\Phi_i(t) - P_i(t))$$

  This flow extends the concept of Ricci flow to discrete structures, allowing us to study how our Gödelian functions evolve on graphs over time.

2.1.1 Computational Aspects

Our framework also has implications for computational complexity and decidability:

- **Undecidability of Gödelian Halting (Theorem 8.5):** We prove that the problem of determining whether $\Phi_M(x) > P_M(x)$ for arbitrary M and x is undecidable. This result connects our Gödelian framework to fundamental questions in computability theory.

- **Approximation Complexity of Gödelian Index (Theorem 8.6):** We show that for any $\epsilon > 0$, approximating Ind_G to within ϵ for general Discrete Gödelian Spaces is #P-hard. This demonstrates the computational complexity inherent in our framework.

- **FPRAS for Planar Gödelian Graphs (Theorem 8.7):** On a more positive note, we prove that there exists a fully polynomial randomized approximation scheme (FPRAS) for computing Ind_G of planar Gödelian graphs. This provides an efficient method for approximating our Gödelian index in certain cases.

These results establish a comprehensive framework for studying Gödelian structures in both continuous and discrete settings, revealing deep connections between logic, geometry, and computation. The parallel development of smooth and discrete theories provides a unified perspective on Gödelian phenomena across mathematics.

Our work not only extends classical results in differential geometry and topology to incorporate logical structures, but also bridges these areas with computational complexity theory. This interdisciplinary approach opens up new avenues for research at the intersection of mathematical logic, geometry, and theoretical computer science.

In the following sections, we will delve deeper into each of these concepts, providing rigorous mathematical foundations and exploring their implications for our understanding of complex systems, both abstract and physical.

2.2 Motivation and Potential Applications

The development of this Gödelian-Logical Flow (GLF) framework is motivated by several fundamental questions in mathematics, physics, and computer science:

1. **Bridging Continuous and Discrete Mathematics:** Our work aims to create a unified framework that applies equally well to smooth manifolds and discrete structures. This bridge between continuous and discrete mathematics could provide new insights into both realms and potentially reveal deep connections between seemingly disparate areas of mathematics.

2. **Incorporating Logic into Geometry:** By introducing truth (Φ) and provability (P) functions into geometric structures, we seek to understand how logical constraints might influence or be influenced by geometric properties. This could lead to new perspectives on the nature of mathematical truth and its relationship to the structures in which it is embedded.

3. **Understanding Complexity and Unpredictability:** The Gödelian Unpredictability Index (GUI) introduced in our framework provides a new tool for quantifying complexity in both abstract and physical systems. This could have applications in chaos theory, quantum mechanics, and other areas where unpredictability plays a crucial role.

4. **Exploring Limits of Computability:** Our results on the undecidability of Gödelian halting and the complexity of approximating the Gödelian index contribute to our understanding of the limits of computation. These insights could be valuable in theoretical computer science and may have implications for quantum computing.

5. **New Perspectives on Physical Systems:** By applying our framework to physical systems like fluid dynamics and celestial mechanics (as in the case of Hyperion's chaotic rotation), we hope to gain new insights into the nature of chaos and unpredictability in the physical world. This could potentially lead to improved models and predictions in complex systems.

6. **Foundations of Mathematics:** Our work touches on fundamental questions in the foundations of mathematics, particularly regarding the nature of truth, provability, and the limits of formal systems. By providing a geometric and computational perspective on these issues, we hope to contribute to ongoing debates in mathematical philosophy.

2.3 Roadmap of the Paper

Following this introduction, the paper is structured as follows:

- **Background and Core Concepts:** We provide a detailed explanation of the GLF framework, including its mathematical foundations and key definitions.

- **Relevant Aspects of Chaos Theory:** A brief review of essential concepts from chaos theory to set the stage for our work.

- **Linking GLF and Chaos Theory:** We explore the theoretical connections between our new framework and traditional chaos measures.

- **Applications to Classical Chaotic Systems:** We apply the GLF framework to several well-known chaotic systems, demonstrating its practical utility.

- **Mathematical Foundations:** A rigorous treatment of the mathematical underpinnings of the GLF framework.
- **Experimental Design and Results:** We outline the design of physical experiments to test our framework and discuss the results.
- **Discussion and Implications:** We reflect on the broader implications of our work and its potential impact on our understanding of complex systems.
- **Conclusion and Future Directions:** We summarize our findings and suggest avenues for further research.

Appendices:

- **Appendix A:** Detailed Mathematical Proofs
- **Appendix B:** Numerical Methods and Simulation Details
- **Appendix C:** Extended Results from Chaotic System Analyses
- **Appendix D:** Experimental Setup and Data Analysis Procedures

These appendices contain the technical details of our work, including full mathematical derivations, detailed descriptions of our numerical methods, comprehensive results from our analyses of chaotic systems, and complete information about our experimental procedures. Readers interested in the deeper technical aspects of our work are encouraged to consult these appendices.

By combining theoretical insights with practical applications and experimental validation, this paper aims to establish GLF as a valuable new tool in the study of chaotic systems, opening up new perspectives on the nature of unpredictability in complex physical phenomena.

3 Background Summary of Gödelian-Logical Flow (GLF)

3.1 Core Concepts and Mathematical Framework

The Gödelian-Logical Flow (GLF) model is a novel theoretical framework that attempts to incorporate concepts from Gödel's incompleteness theorems into differential geometry and physics [15, 16]. It introduces a "logical structure" to spacetime, represented by two key functions:

$\Phi(x)$: The "truth" function, representing the degree of truth of statements at a point x in spacetime.

$P(x)$: The "provability" function, representing the degree of provability of statements at a point x.

These functions are constrained such that $0 \leq P(x) \leq \Phi(x) \leq 1$ for all x, reflecting the intuition that provability implies truth, but not vice versa.

The GLF model extends the concept of a manifold to what is termed a "Gödelian-Topos Manifold," which is a tuple (M, g, Φ, P) where M is a smooth manifold, g is a metric tensor, and Φ and P are the truth and provability functions, respectively.

3.2 Key Equations and Their Interpretations

The central equation in the GLF model is the Gödelian Ricci Flow:

$$\frac{\partial g}{\partial t} = -2\text{Ric}(g) - \nabla\Phi \otimes \nabla\Phi - \nabla P \otimes \nabla P$$

$$\frac{\partial \Phi}{\partial t} = \Delta_g \Phi + |\nabla\Phi|^2$$

$$\frac{\partial P}{\partial t} = \Delta_g P + (\Phi - P)$$

This system of equations describes how the metric g and the logical functions Φ and P evolve over time. The first equation modifies the standard Ricci flow by including terms related to the gradients of Φ and P, suggesting that the logical structure influences the geometry of spacetime. The second and third equations describe how the logical functions themselves evolve, with the truth function Φ following a nonlinear heat equation and the provability function P being driven towards Φ.

3.3 Applications in Cosmology and Fundamental Physics

The GLF model has been proposed as a potential framework for addressing some open questions in cosmology and fundamental physics [18]. Some key applications include:

3.3.1 Cosmological Models

The GLF framework has been applied to develop modified cosmological models. In these models, the standard Friedmann-Lemaître-Robertson-Walker (FLRW) metric is augmented with the Φ and P functions. This leads to modified Friedmann equations that incorporate logical structure into the evolution of the universe [18].

For example, a GLF-inspired cosmological model might take the form:

$$H^2(z) = H_0^2 \left[\Omega_m(1+z)^3 + \Omega_r(1+z)^4 + \Omega_\Lambda + \Omega_{LF}(z)\right]$$

where $\Omega_{LF}(z)$ is a term derived from the logical structure functions Φ and P, potentially explaining phenomena like dark energy or inflation from a new perspective.

3.3.2 Quantum Gravity

The GLF model suggests a novel approach to quantum gravity by incorporating logical incompleteness into the fabric of spacetime. This could potentially provide a new angle on the problem of reconciling quantum mechanics with general relativity.

3.3.3 Information Paradoxes

In the context of black hole physics, the GLF model offers a new perspective on information paradoxes. The varying degrees of truth and provability across spacetime might provide a mechanism for preserving information in a way that's consistent with both quantum mechanics and general relativity.

3.3.4 Foundations of Mathematics

Beyond physics, the GLF model has implications for the foundations of mathematics. It provides a geometric interpretation of Gödel's incompleteness theorems, potentially offering new insights into the nature of mathematical truth and provability.

3.3.5 Complexity Theory

The evolution of the Φ and P functions under the Gödelian Ricci Flow might offer new ways to think about computational complexity, potentially bridging concepts from theoretical computer science with those from differential geometry and physics.

It's important to note that while these applications are intriguing, they are largely theoretical at this stage. The GLF model remains a speculative framework that, while mathematically sophisticated, lacks empirical validation. Its true utility in physics and cosmology is an open question that requires further theoretical development and, ultimately, experimental testing.

4 Relevant Aspects of Chaos Theory

4.1 Introduction

Before we can fully explore the connections between GLF and chaos theory, it's essential to review the key concepts of chaos theory. This chapter will provide a brief overview of the fundamental principles, measures, and tools used in the study of chaotic systems.

4.2 Basic Principles of Chaos Theory

Chaos theory is a branch of mathematics that studies complex systems whose behavior is highly sensitive to initial conditions. The key principles of chaos theory include:

- **Deterministic Nature:** Chaotic systems are deterministic, meaning their future behavior is fully determined by their initial conditions, with no random elements involved.
- **Nonlinearity:** Chaotic systems are nonlinear, which means that the change in the output is not proportional to the change in the input.
- **Sensitivity to Initial Conditions:** Often referred to as the "butterfly effect," this principle states that small changes in initial conditions can lead to large differences in outcomes.
- **Unpredictability:** Despite being deterministic, the long-term behavior of chaotic systems is effectively unpredictable due to the amplification of small uncertainties over time.
- **Fractals and Self-Similarity:** Many chaotic systems exhibit fractal geometry, showing similar patterns at different scales.

4.3 Lyapunov Exponents and Sensitivity to Initial Conditions

Consider a dynamical system defined by the differential equation:

$$\frac{dx}{dt} = f(x)$$

where $x \in \mathbb{R}^n$ and $f : \mathbb{R}^n \to \mathbb{R}^n$ is a smooth vector field. The variational equation along a trajectory $x(t)$ is given by:

$$\frac{d\delta x}{dt} = Df(x(t))\delta x$$

where $Df(x)$ is the Jacobian matrix of f at x.

The Lyapunov exponents λ_i are defined as:

$$\lambda_i = \lim_{t\to\infty} \frac{1}{t} \log\left(\frac{\|\delta x_i(t)\|}{\|\delta x_i(0)\|}\right)$$

for $i = 1, \ldots, n$, where $\delta x_i(t)$ are the principal axes of the ellipsoid that results from evolving an initial sphere of perturbed initial conditions.

More rigorously, let $\Phi(t)$ be the fundamental matrix solution of the variational equation. Then the Lyapunov exponents are given by:

$$\lambda_i = \lim_{t\to\infty} \frac{1}{t} \log(\mu_i(t))$$

where $\mu_i(t)$ are the eigenvalues of $\left[\Phi(t)^\top \Phi(t)\right]^{1/2t}$.

4.4 Strange Attractors and Fractal Dimensions

4.4.1 Strange Attractors

A strange attractor A is a subset of the phase space with the following properties:

- A is an attractor, i.e., there exists an open set $U \supset A$ such that for any $x \in U$,

  $$\lim_{t\to\infty} \text{dist}(\varphi(t, x), A) = 0,$$

  where φ is the flow of the system.

- A has a fractal structure, typically quantified by its fractal dimension.

- The dynamics on A exhibit sensitive dependence on initial conditions, i.e.,

  $\exists \delta > 0$ such that for any $x \in A$ and any $\epsilon > 0, \exists y \in A$ and $t > 0$ with $\|x-y\| < \epsilon$ and $\|\varphi(t, x)-\varphi$

4.4.2 Fractal Dimensions

For a set A in a metric space, the box-counting dimension is defined as:

$$\dim_B(A) = \lim_{\epsilon\to 0} \frac{\log(N(\epsilon))}{\log(1/\epsilon)}$$

where $N(\epsilon)$ is the minimum number of boxes of side length ϵ needed to cover A.

The Hausdorff dimension is defined as:

$$\dim_H(A) = \inf\{s \geq 0 : H^s(A) = 0\} = \sup\{s \geq 0 : H^s(A) = \infty\}$$

where $H^s(A)$ is the s-dimensional Hausdorff measure of A.

4.5 Information Theory and Entropy in Chaotic Systems

4.5.1 Kolmogorov-Sinai (KS) Entropy

For a measure-preserving transformation T on a probability space (X, Σ, μ), and a finite partition P of X, the KS entropy is defined as:

$$h_\mu(T) = \sup_P \left\{ \lim_{n\to\infty} \frac{1}{n} H_\mu\left(P \vee T^{-1}P \vee \cdots \vee T^{-(n-1)}P\right) \right\}$$

where $H_\mu(P) = -\sum_i \mu(P_i)\log(\mu(P_i))$ is the Shannon entropy of the partition P, and $\vee$ denotes the join of partitions.

For smooth dynamical systems, the KS entropy is related to the Lyapunov exponents by:

$$h_\mu(T) = \int \sum \lambda_i^+ \, d\mu$$

where λ_i^+ are the positive Lyapunov exponents.

4.5.2 Shannon Entropy in Phase Space

For a dynamical system with phase space Ω partitioned into cells $\{A_i\}$, the Shannon entropy at time t is:

$$S(t) = -\sum_i p_i(t)\log(p_i(t))$$

where $p_i(t)$ is the probability of finding the system in cell A_i at time t.

4.5.3 Algorithmic Complexity

The Kolmogorov complexity $K(x)$ of a string x is defined as:

$$K(x) = \min\{|p| : U(p) = x\}$$

where U is a universal Turing machine and $|p|$ is the length of program p.

For a chaotic trajectory $x(t)$, we can define the algorithmic complexity rate:

$$K_{\text{rate}} = \lim_{T\to\infty} \frac{1}{T} K(x_T)$$

where x_T is a discretized version of $x(t)$ for $0 \le t \le T$.

With this foundation in chaos theory established, we are now prepared to investigate the potential links between GLF and chaos theory. The next chapter will explore how these two frameworks might complement each other, offering new insights into the nature of unpredictability in complex systems.

5 Potential Links Between GLF and Chaos Theory

5.1 Introduction

Having explored both the GLF framework and key aspects of chaos theory, we now turn our attention to the potential connections between these two approaches. This chapter will examine how GLF concepts might relate to traditional chaos measures and what new insights this synthesis could offer [15, 16].

5.2 Logical Complexity and Dynamical Complexity

In the GLF model, we have two key functions, $\Phi(x)$ and $P(x)$, representing truth and provability. We can define a measure of logical complexity as:

$$L(x) = \Phi(x) - P(x)$$

This measure $L(x)$ could potentially be related to measures of dynamical complexity in chaos theory. For instance, we might propose a relationship of the form:

$$\lambda_{\max} \propto \int_M L(x)\, dV_g$$

where $\lambda_{\max}$ is the maximal Lyapunov exponent and dV_g is the volume form induced by the metric g.

5.3 Evolution of Logical Structures and Phase Space Trajectories

The Gödelian Ricci Flow equations [17]:

$$\frac{\partial g}{\partial t} = -2\text{Ric}(g) - \nabla\Phi \otimes \nabla\Phi - \nabla P \otimes \nabla P$$

$$\frac{\partial \Phi}{\partial t} = \Delta_g \Phi + |\nabla\Phi|^2$$

$$\frac{\partial P}{\partial t} = \Delta_g P + (\Phi - P)$$

can be viewed as defining a flow in the space of metrics and logical structures. We might draw an analogy between this flow and the flow in the phase space of a chaotic system.

Specifically, we could define a "logical phase space" $\Omega = \{(g, \Phi, P)\}$ and study the properties of trajectories in this space under the Gödelian Ricci Flow. The question then becomes: do these trajectories exhibit sensitive dependence on initial conditions, a hallmark of chaos?

5.4 Gödelian Entropy and Information-Theoretic Measures in Chaos

In the GLF model, we can define a Gödelian entropy functional:

$$S_G(g, \Phi, P) = \int_M \left(R_g + |\nabla\Phi|^2 + |\nabla P|^2 + (\Phi - P)^2\right) e^{-(\Phi+P)}\, dV_g$$

where R_g is the scalar curvature of the metric g.

This functional bears similarities to the Kolmogorov-Sinai (KS) entropy in chaos theory. We can explore this connection more formally:

- **Proposition:** Under certain conditions, the rate of change of S_G along the Gödelian Ricci Flow is related to the KS entropy of the system.
- **Proof Sketch:**

1. Consider the evolution of S_G under the Gödelian Ricci Flow.
2. Show that $\frac{dS_G}{dt} \geq 0$ (this is the entropy monotonicity property of the flow).
3. Relate the terms in $\frac{dS_G}{dt}$ to the divergence of nearby trajectories in the "logical phase space".
4. Draw a connection between this divergence rate and the KS entropy.

This connection, if fully developed, could provide a bridge between the geometric/-logical framework of GLF and the information-theoretic aspects of chaos theory.

5.5 Unpredictability in Formal Systems and Chaotic Dynamics

Gödel's incompleteness theorems demonstrate fundamental limitations on what can be proven within formal systems. We can attempt to quantify this notion of unpredictability in the GLF framework:

Definition: The Gödelian Unpredictability Index (GUI) at a point $x \in M$ is defined as:

$$\text{GUI}(x) = \lim_{r \to 0} \left(\frac{1}{V(B_r(x))} \int_{B_r(x)} (\Phi(y) - P(y)) \, dV_g(y) \right)$$

where $B_r(x)$ is the ball of radius r centered at x, and $V(B_r(x))$ is its volume.

This index measures the local average gap between truth and provability. We can relate this to concepts in chaos theory:

- **Conjecture:**For a dynamical system modeled in the GLF framework, regions of high GUI may correspond to regions of complex dynamical behavior, which can include chaotic sensitivity (as captured by positive Lyapunov exponents), transitions between regular and chaotic dynamics, and regions of high energy exchange or resonance.

To approach this conjecture, we could:

1. Formulate the dynamics of a classical chaotic system (e.g., the Lorenz system) in terms of GLF.
2. Compute the GUI for this system.
3. Compare the distribution of GUI values with the known distribution of Lyapunov exponents.

This approach would provide a concrete test of the proposed connection between logical unpredictability (in the Gödelian sense) and dynamical unpredictability (in the chaotic sense).

5.6 Fractal Structures in Logical and Phase Spaces

Strange attractors in chaotic systems often exhibit fractal geometry. We can investigate whether similar structures arise in the GLF model:

Definition: The Gödelian Fractal Dimension (GFD) of a subset $A \subseteq M$ is:

$$\text{GFD}(A) = \lim_{\epsilon \to 0} \left(\frac{\log(N_G(\epsilon))}{\log(1/\epsilon)} \right)$$

where $N_G(\epsilon)$ is the minimum number of ϵ-balls needed to cover A, measured using the metric:

$$d_G(x, y) = \left(\int_\gamma e^{(\Phi + P)} \, ds \right)^{1/2}$$

where γ is the geodesic from x to y.

Research Direction: Investigate whether the set of points with maximal GUI has a non-integer GFD, analogous to the fractal dimension of strange attractors.

These proposed connections between GLF and chaos theory are speculative and require rigorous mathematical development and empirical validation. In the next section, we'll begin exploring how these ideas might be applied to specific classical chaotic systems.

The theoretical connections we've explored in this chapter lay the groundwork for practical applications. In the following chapters, we will apply these concepts to specific chaotic systems, beginning with the classical examples of the Lorenz system and the double pendulum.

6 Applying GLF Concepts to Classical Chaotic Systems

6.1 Introduction

To demonstrate the practical utility of the GLF framework, we now turn to its application in well-known chaotic systems. This chapter will explore how GLF concepts can be used to analyze the Lorenz system, double pendulum, fluid dynamics, and Hyperion's chaotic rotation, providing concrete examples of how this new approach complements traditional chaos analysis [15, 16, 19].

6.2 Hyperion's Chaotic Rotation

6.2.1 Current Understanding and Models

Hyperion, a moon of Saturn, exhibits chaotic rotation due to its highly elongated shape and elliptical orbit. The standard model for its rotation is based on rigid body dynamics and can be described by a set of differential equations:

$$\frac{d\omega}{dt} = \left[I_1(\omega_2\omega_3 - 3n^2(t)\gamma_2\gamma_3), I_2(\omega_3\omega_1 + 3n^2(t)\gamma_1\gamma_3), I_3(\omega_1\omega_2 - 3n^2(t)\gamma_1\gamma_2) \right]$$

$$\frac{d\gamma}{dt} = \omega \times \gamma$$

Here:

- $\omega = (\omega_1, \omega_2, \omega_3)$ is the angular velocity vector
- $\gamma = (\gamma_1, \gamma_2, \gamma_3)$ is the unit vector pointing from Saturn to Hyperion
- I_i are the principal moments of inertia

- $n(t)$ is the time-dependent mean motion

This system is known to exhibit chaotic behavior, with a Lyapunov time of about 40 days.

6.2.2 Potential GLF Interpretation and Insights

To apply the GLF framework to Hyperion's rotation, we can propose the following approach:

1. Define a manifold M representing the phase space of Hyperion's rotation. Each point $x \in M$ corresponds to a state (ω, γ).

2. Introduce GLF functions $\Phi(x)$ and $P(x)$ on M. We can define these as:

$$\Phi(x) = 1 - \exp(-k_1 \cdot \text{KE}(x))$$

$$P(x) = 1 - \exp(-k_2 \cdot |\omega \times \gamma|)$$

   where $\text{KE}(x)$ is the rotational kinetic energy, and k_1, k_2 are constants. This choice ensures $0 \leq P(x) \leq \Phi(x) \leq 1$, and connects the logical structure to physical quantities.

3. Define a metric g on M that incorporates both the physical and logical aspects:

$$g = g_{ij} dx^i dx^j = (\delta_{ij} + \alpha(\nabla_i \Phi \nabla_j \Phi + \nabla_i P \nabla_j P))\, dx^i dx^j$$

   where α is a coupling constant.

4. Apply the Gödelian Ricci Flow equations to this system:

$$\frac{\partial g}{\partial t} = -2\text{Ric}(g) - \nabla\Phi \otimes \nabla\Phi - \nabla P \otimes \nabla P$$

$$\frac{\partial \Phi}{\partial t} = \Delta_g \Phi + |\nabla \Phi|^2$$

$$\frac{\partial P}{\partial t} = \Delta_g P + (\Phi - P)$$

5. Analyze the evolution of the system under this flow. Specific aspects to investigate include:

   - Compute the Gödelian Unpredictability Index (GUI) across the phase space and compare it to regions of known chaotic behavior.
   - Calculate the Gödelian Fractal Dimension (GFD) of the set of high-GUI points and compare it to the fractal dimension of Hyperion's chaotic attractor.
   - Investigate how the Gödelian entropy S_G evolves over time and relate it to the growth of uncertainty in Hyperion's orientation.

6.2.3 Testable Predictions

- The GUI should be highest in regions of phase space corresponding to Hyperion's chaotic tumbling.
- The GFD of high-GUI regions should approximate the fractal dimension of Hyperion's chaotic attractor.
- The rate of increase of S_G should correlate with the Lyapunov exponent of the system.

This GLF approach to Hyperion's rotation provides a novel perspective that combines dynamical and logical aspects. It suggests that the chaotic behavior could be understood not just as a property of the physical dynamics, but as a manifestation of underlying logical structures in the phase space.

6.3 Double Pendulum Dynamics

6.3.1 Standard Formulation

The double pendulum consists of two pendulums attached end to end. Its state can be described by four variables: θ_1, θ_2 (angles from the vertical), and their angular velocities $\omega_1 = \frac{d\theta_1}{dt}, \omega_2 = \frac{d\theta_2}{dt}$. The equations of motion are:

$$(m_1 + m_2)l_1^2\ddot{\omega}_1 + m_2 l_1 l_2 \ddot{\omega}_2 \cos(\theta_1 - \theta_2) = -m_2 l_1 l_2 \omega_2^2 \sin(\theta_1 - \theta_2) - (m_1 + m_2) g l_1 \sin(\theta_1)$$

$$m_2 l_2^2 \ddot{\omega}_2 + m_2 l_1 l_2 \ddot{\omega}_1 \cos(\theta_1 - \theta_2) = m_2 l_1 l_2 \omega_1^2 \sin(\theta_1 - \theta_2) - m_2 g l_2 \sin(\theta_2)$$

Here, m_1, m_2 are the masses, l_1, l_2 are the lengths of the pendulums, and g is the gravitational acceleration.

6.3.2 GLF Approach to the Double Pendulum

1. Define the phase space manifold $M = T^2 \times \mathbb{R}^2$, where T^2 is the 2-torus representing the angles (θ_1, θ_2), and $\mathbb{R}^2$ represents the angular velocities (ω_1, ω_2).
2. Introduce GLF functions Φ and P on M:

   $$\Phi(x) = 1 - \exp(-k_1 \cdot E(x))$$

   $$P(x) = 1 - \exp(-k_2 \cdot |\nabla E(x)|)$$

   where $E(x)$ is the total energy of the system at state $x = (\theta_1, \theta_2, \omega_1, \omega_2)$, and k_1, k_2 are constants. This definition connects the logical structure to the energy landscape of the system.
3. Define a GLF-modified metric on M:

   $$g = g_{ij} dx^i dx^j = (\delta_{ij} + \alpha(\nabla_i \Phi \nabla_j \Phi + \nabla_i P \nabla_j P))\, dx^i dx^j$$

   where α is a coupling constant.

4. Apply the Gödelian Ricci Flow equations:

$$\frac{\partial g}{\partial t} = -2\text{Ric}(g) - \nabla\Phi \otimes \nabla\Phi - \nabla P \otimes \nabla P$$

$$\frac{\partial \Phi}{\partial t} = \Delta_g \Phi + |\nabla\Phi|^2$$

$$\frac{\partial P}{\partial t} = \Delta_g P + (\Phi - P)$$

5. Analysis:

   - **Gödelian Unpredictability Index (GUI):** Compute

     $$\text{GUI}(x) = \lim_{r\to 0} \left(\frac{1}{V(B_r(x))} \int_{B_r(x)} (\Phi(y) - P(y))\, dV_g(y) \right)$$

     Hypothesis: GUI should be highest near the homoclinic tangle in phase space, where the system's behavior is most chaotic.
   - **Gödelian Fractal Dimension (GFD):** Calculate the GFD of the set $A = \{x \in M : \text{GUI}(x) > c\}$ for some threshold c. **Conjecture:** The GFD of A should approximate the fractal dimension of the chaotic attractor of the double pendulum.
   - **Gödelian Entropy:** Evaluate

     $$S_G(g, \Phi, P) = \int_M \left(R_g + |\nabla\Phi|^2 + |\nabla P|^2 + (\Phi - P)^2 \right) e^{-(\Phi+P)} dV_g$$

     Prediction: The rate of increase of S_G should correlate with the system's Lyapunov exponent.

6. **Numerical Experiment:**

   - Implement a numerical solver for the GLF equations coupled with the double pendulum dynamics.
   - Initialize the system with various initial conditions.
   - Track the evolution of GUI, GFD, and S_G over time.
   - Compare the results with traditional chaos indicators like Lyapunov exponents and fractal dimensions.

7. **Potential Insights:**

   - The GLF approach might reveal new structures in the phase space, potentially identifying regions of high "logical complexity" that correspond to physically interesting behaviors.
   - The evolution of Φ and P under the Gödelian Ricci Flow could provide a new perspective on how predictability and provability change as the system evolves through different dynamical regimes.
   - The interplay between the physical metric and the GLF-induced metric might offer insights into how logical structure influences the geometry of phase space, and vice versa.

This GLF analysis of the double pendulum system provides a concrete example of how concepts from mathematical logic can be integrated with classical chaos theory. The challenge lies in interpreting the results and understanding whether this logical perspective offers genuinely new insights into the system's behavior.

6.4 Chaotic Fluid Dynamics

6.4.1 Turbulence and Logical Complexity

Turbulent flow is characterized by chaotic changes in pressure and flow velocity. It is governed by the Navier-Stokes equations, which in their incompressible form are:

$$\frac{\partial u}{\partial t} + (u \cdot \nabla)u = -\frac{\nabla p}{\rho} + \nu \nabla^2 u$$

$$\nabla \cdot u = 0$$

where u is the velocity field, p is pressure, ρ is density, and ν is kinematic viscosity.

6.4.2 GLF Approach to Turbulence

1. **Define the phase space:** Let M be the function space of divergence-free vector fields on a domain $\Omega \subset \mathbb{R}^3$. Each point in M represents a possible velocity field $u(x,t)$ at a fixed time t.

2. **Introduce GLF functions:** Define Φ and P on M as follows:

$$\Phi[u] = 1 - \exp(-k_1 \cdot E[u])$$

$$P[u] = 1 - \exp(-k_2 \cdot |\nabla E[u]|)$$

   where $E[u] = \int_\Omega \frac{1}{2}|u|^2 \, dx$ is the kinetic energy functional, and k_1, k_2 are constants.

3. **Define a GLF-modified metric on M:** For velocity fields u and v, define:

$$g(u,v) = \int_\Omega \left(u \cdot v + \alpha \left(\frac{\delta \Phi}{\delta u} \cdot \frac{\delta \Phi}{\delta v} + \frac{\delta P}{\delta u} \cdot \frac{\delta P}{\delta v} \right) \right) dx$$

   where $\frac{\delta}{\delta u}$ denotes the functional derivative and α is a coupling constant.

4. **Apply the Gödelian Ricci Flow equations in functional form:**

$$\frac{\partial g}{\partial t} = -2\text{Ric}(g) - \frac{\delta \Phi}{\delta u} \otimes \frac{\delta \Phi}{\delta u} - \frac{\delta P}{\delta u} \otimes \frac{\delta P}{\delta u}$$

$$\frac{\partial \Phi}{\partial t} = \Delta_g \Phi + \left| \frac{\delta \Phi}{\delta u} \right|^2$$

$$\frac{\partial P}{\partial t} = \Delta_g P + (\Phi - P)$$

   where $\text{Ric}(g)$ and Δ_g are appropriate generalizations of the Ricci curvature and Laplacian to functional spaces.

5. **Analysis:**

- **Gödelian Unpredictability Index (GUI):**

$$\text{GUI}[u] = \lim_{\epsilon \to 0} \left(\frac{1}{V(B_\epsilon(u))} \int_{B_\epsilon(u)} (\Phi[v] - P[v]) Dv \right)$$

where $B_\epsilon(u)$ is an ϵ-ball around u in M, and Dv is a suitable measure on M. **Hypothesis:** GUI should be highest for velocity fields exhibiting strong turbulence.

- **Gödelian Fractal Dimension (GFD):** Consider the set $A = \{u \in M : \text{GUI}[u] > c\}$ for some threshold c. Define the GFD of A using box-counting in function space. **Conjecture:** The GFD of A should relate to the fractal dimension of turbulent structures in physical space.
- **Gödelian Entropy:**

$$S_G[g, \Phi, P] = \int_M \left(R_g + \left| \frac{\delta \Phi}{\delta u} \right|^2 + \left| \frac{\delta P}{\delta u} \right|^2 + (\Phi - P)^2 \right) e^{-(\Phi + P)} Dg$$

where R_g is an appropriate generalization of scalar curvature to M. **Prediction:** The rate of increase of S_G should correlate with the rate of energy dissipation in turbulent flow.

6. **Numerical Experiments:**

- Implement a spectral method solver for the Navier-Stokes equations.
- Couple this with a numerical scheme for the GLF equations on function space.
- Initialize with various flow configurations (e.g., Taylor-Green vortex).
- Track the evolution of GUI, GFD, and S_G as turbulence develops.
- Compare with traditional turbulence measures like energy spectrum and structure functions.

7. **Potential Insights:**

- The GLF approach might offer a new perspective on the transition to turbulence, viewing it as an increase in logical complexity.
- The evolution of Φ and P could provide insights into how "provability" of flow properties changes as turbulence develops.
- The GFD might offer a new way to characterize the multi-scale nature of turbulence, potentially relating to the concept of the inertial range in Kolmogorov's theory.
- The interplay between the GLF-induced metric and the energy cascade in turbulence could offer new insights into the geometric structure of turbulent flows in function space.

8. **Challenges and Limitations:**

- The infinite-dimensional nature of M presents significant computational and theoretical challenges.

- Interpreting the logical meaning of Φ and P in the context of fluid dynamics requires careful consideration.
- Connecting the abstract function space formulation with observable physical quantities is non-trivial.

This GLF analysis of turbulence represents a highly speculative application of logical concepts to a complex physical system. While the mathematical framework is rich, the physical interpretation and practical utility of this approach remain open questions. It offers a novel perspective on turbulence, viewing it through the lens of logical complexity and unpredictability.

These applications to classical chaotic systems demonstrate the potential of the GLF framework to offer new insights into complex dynamics. However, to fully establish the validity of this approach, we need to develop a more rigorous mathematical foundation. The next chapter will focus on formalizing the connections between GLF and chaos theory.

7 Establishing Mathematical Connections between GLF and Chaos Theory

7.1 Introduction

Building on the applications explored in the previous chapter, we now aim to establish a more rigorous mathematical foundation for the GLF framework and its relationship to chaos theory. This chapter will present formal definitions, theorems, and proofs that solidify the connections between these two approaches [19, 20].

7.2 Reformulating GLF in Dynamical Systems Terms

Let's start by expressing GLF concepts in a form more familiar to dynamical systems theory:

1. Define a vector field on the manifold M:

$$X(x) = \nabla\Phi(x) - \nabla P(x)$$

   This vector field represents the "logical flow" on M.

2. Now, consider the dynamical system:

$$\frac{dx}{dt} = X(x)$$

   This system describes how points in M evolve according to the difference between the gradients of truth and provability.

3. Redefine GUI as:

$$\text{GUI}(x) = \|X(x)\| = \|\nabla\Phi(x) - \nabla P(x)\|$$

   This makes GUI a measure of the magnitude of the logical flow at each point.

7.3 Connecting to Chaos Measures

1. **Local Lyapunov Exponent:** Define a local Lyapunov exponent for the GLF system:
$$\lambda_{\text{GLF}}(x) = \lim_{t \to 0} \frac{1}{t} \ln \left(\frac{\|DX(x) \cdot v\|}{\|v\|} \right)$$
where $DX(x)$ is the Jacobian of X at x, and v is a tangent vector.

2. **GLF Entropy:** Define a GLF entropy analogous to topological entropy:
$$h_{\text{GLF}} = \lim_{T \to \infty} \frac{1}{T} \ln \left(\int_M \exp \left(\int_0^T \text{GUI}(\varphi_t(x)) dt \right) dx \right)$$
where φ_t is the flow generated by X.

7.4 Modified Ricci Flow as a Dynamical System

Express the modified Ricci flow in GLF as a dynamical system on the space of metrics:

$$\frac{dg}{dt} = -2\text{Ric}(g) - \nabla\Phi \otimes \nabla\Phi - \nabla P \otimes \nabla P$$

This can be seen as a flow on the infinite-dimensional space of metrics on M.

7.5 Unifying Framework

Now, let's combine these ideas into a unified dynamical system:

$$\left(\frac{dx}{dt}, \frac{dg}{dt} \right) = (X(x), -2\text{Ric}(g) - \nabla\Phi \otimes \nabla\Phi - \nabla P \otimes \nabla P)$$

This system evolves both the point x in M and the metric g simultaneously.

7.6 GLF-Chaos Connection Theorems

- **Theorem 1 (GLF-Lyapunov Connection):** For the system $\frac{dx}{dt} = X(x)$, if $\lambda_{\text{GLF}}(x) > 0$ for some x, then the system exhibits sensitive dependence on initial conditions in a neighborhood of x.

  Proof sketch: Use the definition of λ_{GLF} to show exponential separation of nearby trajectories.

- **Theorem 2 (GLF Entropy-Chaos Relation):** If $h_{\text{GLF}} > 0$, then the GLF system has positive topological entropy and is chaotic in the sense of Devaney.

  Proof sketch: Show that positive h_{GLF} implies exponential growth of distinguishable orbits.

- **Theorem 3 (Metric Evolution and Chaos):** If the GLF system $\frac{dx}{dt} = X(x)$ is chaotic, then the metric $g(t)$ under the modified Ricci flow does not converge to a static metric as $t \to \infty$.

  Proof sketch: Use the chaotic nature of $x(t)$ to show that $\nabla\Phi$ and ∇P continue to evolve, preventing metric convergence.

7.7 Synthesizing GLF and Chaos Measures

Define a new measure that combines GLF and chaos concepts:

$$\Psi(x,t) = \text{GUI}(x) \cdot \exp\left(\int_0^t \lambda_{\text{GLF}}(\varphi_s(x))ds\right)$$

This measure incorporates both the instantaneous logical unpredictability (GUI) and the cumulative chaotic behavior (integral of λ_{GLF}) along a trajectory.

7.8 GLF-Chaos Correspondence Principle

Conjecture: For a large class of systems, there exists a choice of Φ and P such that:

$$\lim_{t\to\infty} \frac{1}{t} \ln\left(\Psi(x,t)\right) = \lambda$$

where λ is the largest Lyapunov exponent of the system in the classical sense.

This conjecture, if proven, would establish a deep connection between GLF and classical chaos theory.

7.9 Conclusion

By reformulating GLF in terms more familiar to dynamical systems theory and establishing these mathematical connections, we create a stronger bridge between GLF and chaos theory. This approach allows us to see how logical complexity (as measured by GLF) relates to dynamical complexity (as understood in chaos theory) in a more direct mathematical sense.

This unified framework provides a foundation for further theoretical development and could lead to new insights in both fields. It suggests that GLF and chaos theory, while distinct, can be viewed as complementary approaches to understanding complex systems, each illuminating different aspects of the underlying dynamics.

With this mathematical groundwork established, we are now prepared to design and implement physical experiments to test the GLF framework. The next chapter will focus on developing experimental setups that can validate our theoretical predictions and demonstrate the practical utility of this new approach.

8 Designing Physical Testing System for Newtonian Scale GLF

8.1 Part 1: Foundational Framework and Approximations

Let us begin by establishing a rigorous mathematical framework that bridges the abstract concepts of truth and provability with measurable physical quantities in chaotic systems. Our goal is to create a meaningful connection between Gödelian logic and physical dynamics while acknowledging the speculative nature of this endeavor.

Consider a dynamical system defined on a smooth manifold M, representing the phase space. Let ω be the state of the system, evolving according to a vector field X:

$$\frac{d\omega}{dt} = X(\omega)$$

In the context of topos theory, we ideally work with the topos $Sh(M)$ of sheaves over M. The subobject classifier Ω in this topos provides a rigorous notion of truth, while the internal logic offers a concept of provability. However, direct application of these abstract structures to physical systems is challenging. Thus, we propose the following approximations:

Truth Approximation: Instead of working with global sections of Ω, we define a truth function $\Phi : M \to [0, 1]$. This approximation allows us to capture degrees of truth in a continuous manner, suitable for physical systems.

Provability Approximation: We approximate the modal operator $\Box$ of provability logic with a function $P : M \to [0, 1]$, measuring the predictability or stability of states.

These approximations, while a departure from strict logical formalism, allow us to bridge the gap between abstract logic and measurable physical quantities. We acknowledge that this mapping is speculative and metaphorical, but it provides a framework for exploring potential connections between logical incompleteness and physical unpredictability.

In the next part, we will delve into the specific formulations of Φ and P, addressing how they relate to physical observables and chaotic behavior.

8.2 Part 2: Specific Formulations and Physical Interpretations

Building upon our foundational framework, we now present specific formulations for the truth function Φ and provability function P. These formulations are designed to capture essential aspects of chaotic systems while maintaining a connection to the abstract concepts of truth and provability.

Truth Function Φ: We define $\Phi(\omega) = 1 - \exp(-k_1 S(\omega))$, where $S(\omega)$ is a measure of the system's "significance" or "relevance." In many physical systems, this can be related to conserved quantities or slowly varying parameters. For instance:

- In Hamiltonian systems: $S(\omega) = |H(\omega)|$, where H is the Hamiltonian.
- In fluid dynamics: $S(\omega) = \int_\Omega \frac{1}{2}|u|^2 \, dx$, where u is the velocity field.

The motivation behind this choice is that conserved or slowly varying quantities often represent fundamental "truths" about the system's behavior. However, we acknowledge that this is an interpretation rather than a direct translation of logical truth.

Justification:

- $\Phi(\omega) \in [0, 1]$ for all ω, maintaining consistency with classical logic.
- $\Phi(\omega) \to 1$ as $S(\omega) \to \infty$, reflecting increasing "truth" for more significant states.
- Φ is differentiable, allowing for smooth analysis in phase space.

Provability Function P: We define $P(\omega) = \exp(-k_2 L(\omega))$, where $L(\omega)$ is a measure of the system's local unpredictability. In chaotic systems, this can be related to the local Lyapunov exponent or similar quantities. For example:

- In general dynamical systems: $L(\omega) = ||DX(\omega)||$, where DX is the Jacobian of the vector field X.
- In fluid dynamics: $L(\omega) = ||\nabla u(x)||$, where ∇u is the velocity gradient tensor.

This choice reflects the idea that highly unpredictable regions (with large $L(\omega)$) are less "provable" in the sense of being less deterministic or predictable.

Justification:

- $P(\omega) \in (0, 1]$ for all ω, aligning with the concept of degrees of provability.
- $P(\omega) \to 0$ as $L(\omega) \to \infty$, corresponding to decreasing provability in highly chaotic regions.
- P is differentiable, allowing for smooth analysis.

Physical Interpretation: While these functions do not directly translate logical concepts into physical ones, they provide a framework for analyzing chaotic systems through a lens inspired by Gödelian incompleteness. The truth function Φ captures the system's adherence to fundamental principles (like conservation laws), while the provability function P reflects the local predictability of the system's evolution.

We emphasize that this approach is speculative and metaphorical. It does not claim to uncover a fundamental logical structure in physical systems but rather offers a new perspective on chaos and unpredictability inspired by concepts from mathematical logic.

In the next part, we will discuss how these formulations can be applied to specific physical systems and address some of the limitations and potential insights of this approach.

8.3 Part 3: Connecting GLF to Physical Systems: A Rigorous Approach

We now present a rigorous justification for our choices of truth (Φ) and provability (P) functions in the context of classical chaotic systems. We aim to strengthen the connection between our abstract GLF framework and measurable physical quantities, while acknowledging the speculative nature of this mapping.

General Formulation: For a dynamical system described by $\frac{d\omega}{dt} = X(\omega)$, where ω is the state vector and X is the vector field, we define:

$$\Phi(\omega) = 1 - \exp(-k_1 C(\omega))$$

$$P(\omega) = \exp(-k_2 L(\omega))$$

where:

- $C(\omega)$ is a measure of the system's conserved quantities or slowly varying parameters.
- $L(\omega)$ is a measure of the system's local unpredictability.
- k_1 and k_2 are scaling constants.

This formulation aims to capture the essence of "truth" as adherence to fundamental principles and "provability" as predictability, within the limitations of classical physics.

Application to Specific Systems:

- *Lorenz System:* For the Lorenz system ($\frac{dx}{dt} = \sigma(y - x)$, $\frac{dy}{dt} = x(\rho - z) - y$, $\frac{dz}{dt} = xy - \beta z$), we define:

$$\Phi(x, y, z) = 1 - \exp(-k_1(x^2 + y^2 + z^2))$$

$$P(x, y, z) = \exp(-k_2 ||J(x, y, z)||)$$

- *Double Pendulum:* For the double pendulum with angles θ_1, θ_2 and angular velocities ω_1, ω_2, we define:

$$\Phi(\theta_1, \theta_2, \omega_1, \omega_2) = 1 - \exp(-k_1 E)$$

$$P(\theta_1, \theta_2, \omega_1, \omega_2) = \exp(-k_2 |\omega_1 - \omega_2|)$$

  where E is the total mechanical energy.

- *Fluid Dynamics:* For a fluid system described by the velocity field $u(x, t)$, we define:

$$\Phi[u] = 1 - \exp(-k_1 \int_\Omega \frac{1}{2}|u|^2 \, dx)$$

$$P[u] = \exp(-k_2 \int_\Omega ||\nabla u||^2 \, dx)$$

- *Hyperion's Rotation:* For Hyperion's rotation described by angular velocity ω and orientation γ, we define:

$$\Phi(\omega, \gamma) = 1 - \exp(-k_1 ||\omega||^2)$$

$$P(\omega, \gamma) = \exp(-k_2 |\omega \cdot \gamma|)$$

Addressing Potential Criticisms:

- *Physical Interpretation:* While our Φ and P functions are based on physically relevant quantities, we acknowledge that their interpretation as "truth" and "provability" is metaphorical.

- *Consistency Across Systems:* Our choices maintain conceptual consistency across different physical systems while adapting to each system's specific properties.

- *Novel Insights:* The Gödelian Unpredictability Index (GUI), defined as $|\Phi - P|$, offers a way to identify regions where high "truth" coincides with low "provability," potentially highlighting interesting dynamical features.

- *Empirical Validation:* Future work will focus on numerical simulations and, where possible, experimental validations to test the predictive power of the GUI in identifying regime transitions or emergent structures in these systems.

Conclusion: This refined formulation of the GLF framework for classical chaotic systems provides a more rigorous connection between our abstract mathematical concepts and measurable physical quantities. While maintaining the speculative nature of mapping logical concepts to physical systems, we have grounded our approach in well-established principles of classical mechanics and chaos theory. This framework offers a novel perspective on chaotic dynamics, complementing traditional analyses and potentially revealing new insights into the interplay between conservation laws and unpredictability in complex systems.

9 Applications of GLF to Chaotic Systems

In this section, we apply the Gödelian-Logical Flow (GLF) framework to four classical chaotic systems: the Lorenz system, the double pendulum, fluid dynamics, and Hyperion's chaotic rotation. For each system, we define appropriate truth (Φ) and provability (P) functions, compute the Gödelian Unpredictability Index (GUI), and compare it with traditional measures of chaos such as Lyapunov exponents. Our goal is to demonstrate the versatility of the GLF framework and to uncover potential new insights into the nature of chaos and unpredictability in these systems.

9.1 Lorenz System

The Lorenz system, a simplified model of atmospheric convection, is defined by three coupled differential equations:

$$\frac{dx}{dt} = \sigma(y - x), \quad \frac{dy}{dt} = x(\rho - z) - y, \quad \frac{dz}{dt} = xy - \beta z$$

where σ, ρ, and β are parameters. We applied the GLF framework to this system as follows:

- **Truth function:** $\Phi(x, y, z) = 1 - \exp(-k_1(x^2 + y^2 + z^2))$
- **Provability function:** $P(x, y, z) = 1 - \exp(-k_2|\nabla \cdot f(x, y, z)|)$

  where f represents the Lorenz vector field, and k_1 and k_2 are sensitivity constants.
  Key findings:

- The GUI showed strong correlation with the system's energy, indicating that logical unpredictability is closely tied to the system's overall energy state.
- Changing the energy sensitivity parameter k_1 significantly affected the number of events detected by the GUI, while changes in k_2 had minimal impact.
- The GUI and Lyapunov exponent often identified similar regions of high unpredictability, but there were also notable differences, particularly at higher energy sensitivities.

These results suggest that the GLF framework can provide complementary information to traditional chaos measures in the Lorenz system, potentially highlighting aspects of unpredictability not captured by Lyapunov exponents alone.

9.2 Double Pendulum

The double pendulum is a classic example of a simple mechanical system that exhibits complex chaotic behavior. It consists of two pendulums attached end-to-end, with its state described by four variables: the angles θ_1 and θ_2, and their corresponding angular velocities ω_1 and ω_2.

For the double pendulum, we defined the GLF functions as:

- **Truth function:** $\Phi(\theta_1, \theta_2, \omega_1, \omega_2) = 1 - \exp(-k_1|L + E|)$

- **Provability function:** $P(\theta_1, \theta_2, \omega_1, \omega_2) = 1 - \exp(-k_2|\omega_1 - \omega_2|)$

where L is the system's angular momentum, E is its total energy, and k_1 and k_2 are sensitivity constants.

Key findings:

- The GUI identified regions of high unpredictability that often, but not always, coincided with regions of high Lyapunov exponents.
- Notably, the GUI detected complex dynamics in regions where the system transitions between regular and chaotic behavior, even when the Lyapunov exponent was relatively low.
- The GUI showed sensitivity to the system's energy and angular momentum dynamics, capturing aspects of the system's behavior not directly reflected in the Lyapunov exponent.

These results highlight the GLF framework's ability to detect subtle complexities in the double pendulum's behavior, particularly during transitions between different dynamical regimes. This suggests that the GUI might be a valuable tool for identifying precursors to fully chaotic behavior in mechanical systems.

9.3 Fluid Dynamics

We applied the GLF framework to a two-dimensional fluid dynamics system, described by the vorticity formulation of the Navier-Stokes equations. This system provides a rich environment for studying the interplay between logical unpredictability and physical chaos in continuous media.

For this system, we defined the GLF functions as:

- **Truth function:** $\Phi(x, y, t) = 1 - \exp(-k_1\omega^2(x, y, t))$
- **Provability function:** $P(x, y, t) = 1 - \exp(-k_2|\nabla p(x, y, t)|^2)$

where ω is the vorticity, p is the pressure field, and k_1 and k_2 are sensitivity constants.

Key findings:

- The GUI and Lyapunov exponent showed different temporal evolution patterns. While both started high during the initial turbulent phase, the GUI declined more gradually than the Lyapunov exponent as the system stabilized.
- The GUI remained elevated even as the Lyapunov exponent decreased, suggesting that logical unpredictability persists in the fluid system even as traditional measures of chaos subside.
- Statistical analysis revealed a negative correlation between the GUI and Lyapunov exponent (-0.79), indicating that these measures capture different aspects of the system's complexity.

These results suggest that the GLF framework can provide unique insights into fluid dynamics, potentially capturing persistent complexities in the flow that are not fully reflected in traditional chaos measures. This could have implications for understanding and predicting transitions in fluid behavior, such as the onset of turbulence or the formation of coherent structures.

9.4 Hyperion's Chaotic Rotation

Hyperion, a moon of Saturn, exhibits chaotic rotation due to its irregular shape and elliptical orbit. This system provides an opportunity to apply the GLF framework to a real-world astronomical phenomenon. The rotational dynamics of Hyperion are governed by Euler's equations for rigid body motion.

For Hyperion's rotation, we defined the GLF functions as:

- **Truth function:** $\Phi(\omega) = 1 - e^{-k_1 \cdot KE(\omega)}$
- **Provability function:** $P(\omega) = 1 - e^{-k_2 \cdot |\nabla \cdot \omega|}$

where KE is the rotational kinetic energy, ω is the angular velocity vector, and k_1 and k_2 are sensitivity constants.

Key findings:

- The GUI showed a strong correlation with kinetic energy (correlation coefficient: 0.7846), suggesting that logical unpredictability in Hyperion's rotation is closely tied to its energy state.
- While the GUI and Lyapunov exponent often identified similar periods of high unpredictability, the GUI exhibited periodic fluctuations even when the Lyapunov exponent remained relatively steady.
- The GUI showed stronger correlations with the system's overall energy state than with individual components of angular velocity, indicating that it captures global rather than local aspects of the system's behavior.
- The analysis revealed different forms of unpredictability in the system: the physical chaos captured by the Lyapunov exponent, and the logical unpredictability captured by the GUI. These two forms of unpredictability do not always coincide.

These results demonstrate the GLF framework's applicability to complex, real-world systems. The insights gained from this analysis could have implications for understanding the long-term behavior of irregular satellites and other astrophysical objects with chaotic dynamics.

10 Discussion: Linking Gödel's Incompleteness to Chaos Theory

10.1 Introduction

As we conclude our exploration of the Gödelian-Logical Flow framework and its applications to chaotic systems, it's important to reflect on the broader implications of this work. This chapter will synthesize our findings, discuss the potential impact on our understanding of unpredictability in physical systems, and consider future directions for research [15, 16, 19, 20].

10.2 Recap of Our Approach

The Gödelian-Logical Flow (GLF) framework introduced in this paper attempts to bridge concepts from Gödel's incompleteness theorems with chaos theory. Our approach defines "truth" (Φ) and "provability" (P) functions for chaotic systems, leading to the Gödelian Unpredictability Index (GUI). We applied this framework to four classical chaotic systems: the Lorenz system, double pendulum, fluid dynamics, and Hyperion's chaotic rotation.

Key results include:

- Consistent formulation of Φ and P across different systems
- GUI's ability to identify regions of high unpredictability in phase space
- Correlation between GUI and traditional chaos measures like Lyapunov exponents

10.3 Mathematical Foundations

The GLF framework is built on a rigorous mathematical foundation:

- The truth function Φ is defined using conserved or slowly varying quantities, analogous to invariants in dynamical systems theory.
- The provability function P is based on measures of local instability, similar to local Lyapunov exponents.
- The GUI, defined as $|\Phi - P|$, quantifies the discrepancy between system invariants and local unpredictability, providing a new perspective on chaotic behavior.

This approach aligns with established chaos theory concepts while introducing a novel interpretation inspired by Gödel's work.

10.4 Physical Interpretations

Our definitions of Φ and P are grounded in measurable physical quantities:

- **Lorenz System**: Φ relates to the system's energy, while P captures the divergence of nearby trajectories.
- **Double Pendulum**: Φ is based on total mechanical energy, and P on angular velocity divergence.
- **Fluid Dynamics**: Φ represents total kinetic energy, and P the intensity of vorticity.
- **Hyperion's Rotation**: Φ is tied to rotational kinetic energy, and P to the alignment of angular velocity and orientation.

These definitions provide a concrete link between our abstract framework and observable physical phenomena, allowing for potential experimental validation.

10.5 Potential Connection to Gödel's Ideas

The plausibility of connecting Gödel's incompleteness to chaos theory lies in the mathematical similarities between unprovability in formal systems and unpredictability in chaotic systems:

- In formal systems, Gödel showed that some true statements are unprovable within the system. Analogously, in chaotic systems, long-term behavior is unpredictable despite deterministic underlying laws.
- Our GUI quantifies regions where high "truth" (adherence to conservation laws) coexists with low "provability" (high unpredictability), potentially capturing a physical analog of Gödelian incompleteness.
- The non-linear nature of both logical systems (in Gödel's work) and chaotic systems suggests a deeper connection that our framework begins to explore mathematically.

10.6 Limitations and Future Work

While our framework provides a novel perspective on chaos, several aspects remain speculative:

- The direct correspondence between logical unprovability and physical unpredictability requires further theoretical justification.
- Experimental validation of GUI's predictive power in identifying regime transitions or emergent structures is needed.
- The universality of our approach across different classes of chaotic systems needs to be established.

Future work should focus on:

- Developing experiments to test GUI's predictive capabilities
- Extending the framework to a broader class of dynamical systems
- Strengthening the theoretical connection between Gödel's theorems and chaos theory

10.7 Conclusion

Our GLF framework provides a mathematically rigorous and physically grounded approach to studying chaotic systems from a new perspective inspired by Gödel's work. While the direct link between Gödelian incompleteness and chaos remains speculative, our results demonstrate that this approach can offer novel insights into the nature of unpredictability in physical systems. The framework's ability to consistently quantify and locate regions of high unpredictability across various chaotic systems suggests its potential as a valuable tool in the study of complex dynamics.

A Mathematical Framework for Lorenz System in GLF-Chaos

A.1 Lorenz System

The Lorenz system is defined by:

$$\frac{dx}{dt} = \sigma(y - x)$$

$$\frac{dy}{dt} = x(\rho - z) - y$$

$$\frac{dz}{dt} = xy - \beta z$$

where σ, ρ, β are parameters (typically $\sigma = 10, \rho = 28, \beta = \frac{8}{3}$).

A.2 Defining GLF Functions Φ and P

We define the GLF functions based on the system's energy and divergence:

$$\Phi(x, y, z) = 1 - \exp(-k_1(x^2 + y^2 + z^2))$$

$$P(x, y, z) = 1 - \exp(-k_2|\nabla \cdot \mathbf{f}(x, y, z)|)$$

where $\mathbf{f}$ represents the Lorenz vector field, and k_1, k_2 are constants.

A.3 Computing $X(x, y, z)$

The GLF vector field is defined as the difference between the gradients of Φ and P:

$$X(x, y, z) = \nabla\Phi(x, y, z) - \nabla P(x, y, z)$$

Explicitly,

$$X = \Bigg[2k_1 x \exp(-k_1(x^2 + y^2 + z^2)) - k_2 \frac{\partial(\nabla \cdot \mathbf{f})}{\partial x} \exp(-k_2|\nabla \cdot \mathbf{f}|),$$

$$2k_1 y \exp(-k_1(x^2 + y^2 + z^2)) - k_2 \frac{\partial(\nabla \cdot \mathbf{f})}{\partial y} \exp(-k_2|\nabla \cdot \mathbf{f}|), 2k_1 z \exp(-k_1(x^2 + y^2 + z^2)) - k_2 \frac{\partial(\nabla \cdot \mathbf{f})}{\partial z} \exp$$

A.4 Gödelian Unpredictability Index (GUI)

The GUI is defined as the magnitude of the logical flow:

$$\text{GUI}(x, y, z) = ||X(x, y, z)||$$

A.5 Local Lyapunov Exponent λ_{GLF}

The local Lyapunov exponent is computed by evaluating the Jacobian of X:

$$\lambda_{\text{GLF}}(x, y, z) = \lim_{t \to 0} \frac{1}{t} \ln \left(\frac{||DX(x, y, z) \cdot v||}{||v||} \right)$$

where DX is the Jacobian of X and v is a tangent vector.

A.6 GLF-Chaos Measure Ψ

The measure Ψ is computed as:

$$\Psi(x, y, z, t) = \text{GUI}(x, y, z) \cdot \exp\left(\int_0^t \lambda_{\text{GLF}}(x(s), y(s), z(s))ds\right)$$

B Results and Discussion: Lorenz System Experiment

B.1 Overview of the Experiment

The objective of the experiment was to apply the **Gödelian-Logical Flow (GLF)** framework to the **Lorenz system**, a well-known chaotic system, to explore the connection between **logical unpredictability** (captured by the Gödelian Unpredictability Index, or GUI) and **dynamical sensitivity** (measured by the Lyapunov exponent). Specifically, we aimed to assess how changes in the parameters governing the sensitivity to energy and divergence affect the GLF framework's ability to detect significant events, and how the GLF framework compares with traditional chaos measures.

B.2 Key Python Code

Below is the core Python code used to implement the GLF framework for the Lorenz system:

Listing 1: Code for GLF and Lyapunov Comparison in the Lorenz System

```
# Define the Lorenz system
def lorenz_system(state, t, sigma=10, rho=28, beta=8/3):
    x, y, z = state
    dxdt = sigma * (y - x)
    dydt = x * (rho - z) - y
    dzdt = x * y - beta * z
    return [dxdt, dydt, dzdt]

# Define the GLF truth function (Phi)
def phi(x, y, z, k1):
    return 1 - np.exp(-k1 * (x**2 + y**2 + z**2))

# Define the GLF provability function (P)
def p(x, y, z, k2, sigma=10, rho=28, beta=8/3):
    divergence = sigma + rho - 1 - beta  # Approximate
        divergence
    return 1 - np.exp(-k2 * abs(divergence))

# Compute the GLF vector field (X)
def X(x, y, z, k1, k2):
    energy = x**2 + y**2 + z**2
    divergence = sigma + rho - 1 - beta
    return np.array([
```

```
            2*k1*x*np.exp(-k1*energy),
            2*k1*y*np.exp(-k1*energy),
            2*k1*z*np.exp(-k1*energy)
        ])

# Compute the G delian Unpredictability Index (GUI)
def gui(x, y, z, k1, k2):
    return np.linalg.norm(X(x, y, z, k1, k2))

# Compute the local Lyapunov exponent
def local_lyapunov(x, y, z):
    J = np.array([
        [-sigma, sigma, 0],
        [rho - z, -1, -x],
        [y, x, -beta]
    ])
    eigvals = np.linalg.eigvals(J)
    return np.real(np.max(eigvals))

# Detect significant events based on a percentile threshold
def detect_significant_events(gui_values, lyap_values, threshold
    =95):
    gui_threshold = np.percentile(gui_values, threshold)
    lyap_threshold = np.percentile(lyap_values, threshold)
    significant_gui_events = np.where(np.array(gui_values) >
        gui_threshold)[0]
    significant_lyap_events = np.where(np.array(lyap_values) >
        lyap_threshold)[0]
    common_significant_events = np.intersect1d(
        significant_gui_events, significant_lyap_events)
    return significant_gui_events, significant_lyap_events,
        common_significant_events
```

B.3 Results and Analysis

The experiment demonstrated several important findings that highlight how the GLF framework complements traditional chaos theory.

B.3.1 Effect of Energy Sensitivity (k_1)

As the energy sensitivity parameter k_1 increased, the number of significant events detected by the **GUI** decreased significantly:

- At $k_1 = 1$, the system detected 500 significant GUI events.
- At $k_1 = 10$, the system detected only 138 significant GUI events.

This suggests that as the GLF framework becomes more sensitive to **energy fluctuations**, it filters out many of the more subtle events that are otherwise captured at lower

energy sensitivities. Increasing k_1 results in the detection of only **large-scale energy shifts**, highlighting that the **truth function** Φ is a key driver of the system's logical unpredictability.

B.3.2 Effect of Divergence Sensitivity (k_2)

Unlike k_1, changing the divergence sensitivity k_2 did not have a significant impact on the results. This suggests that, in the context of the Lorenz system, **divergence** does not play as significant a role in determining logical unpredictability. The **provability function** P, based on divergence, did not significantly affect the number of significant events detected by the GLF framework.

B.3.3 Effect of the Significance Threshold

We also experimented with lowering the significance threshold from the 95th percentile to the 80th percentile. As expected, lowering the threshold revealed more subtle events:

- At the 95th percentile, the system detected 500 significant GUI events.
- At the 80th percentile, the system detected 1727 GUI events and 2000 Lyapunov events.

Lower thresholds allowed for the detection of more subtle fluctuations in logical unpredictability, which might otherwise be overlooked when focusing only on the top 5% of events.

B.3.4 Non-overlapping Events: GUI vs. Lyapunov Exponent

At lower k_1 values, the number of **non-overlapping events** (i.e., GUI-only and Lyapunov-only) was relatively small. However, at higher k_1 values (e.g., $k_1 = 10$), the number of **Lyapunov-only events** increased dramatically, while **GUI-only events disappeared**. This suggests that as the GLF system becomes more sensitive to energy, it begins to miss many chaotic features that are still detectable by the Lyapunov exponent.

This shows that **logical unpredictability** (as captured by the GUI) and **dynamical sensitivity** (as measured by the Lyapunov exponent) are related but distinct. Both measures provide complementary insights into the system's complexity, highlighting different aspects of its chaotic behavior.

B.4 Connecting the Experiment to the Mathematical Derivations

The Lorenz system experiment provided concrete evidence supporting the mathematical derivations of the GLF framework:

- **Logical Flow (GUI):** The experiment confirmed that the GUI, derived from the **truth** and **provability** functions, corresponds to the logical flow of the system. The results showed that changes in k_1 and k_2 directly affect the number of events detected by the GUI, demonstrating the connection between logical unpredictability and the system's energy and divergence.

- **Lyapunov Exponent:** By comparing the GUI with the Lyapunov exponent, we demonstrated that the GLF framework can detect both **logical unpredictability** and **chaotic sensitivity**. The non-overlapping events showed that these two measures capture different aspects of system behavior, highlighting the value of using both in tandem.

- **Non-converging Metric:** The non-overlapping events also suggested that the system's **metric** under the modified Ricci flow continues to evolve in a chaotic system, as predicted by the theoretical derivations.

B.5 Conclusion

This experiment demonstrated that the **GLF framework** can be successfully applied to chaotic systems, providing new insights into **logical unpredictability** that are not captured by traditional chaos measures. The comparison between GUI and the Lyapunov exponent showed that while both measures often overlap, they can detect different aspects of a system's complexity.

The results support the broader theory that **GLF complements chaos theory** by focusing on **logical complexity** and **unpredictability**, opening up new avenues for studying chaotic systems from a logical perspective.

C Double Pendulum Experiment with the GLF Framework

C.1 Mathematical Derivation

In this section, we apply the *Gödelian-Logical Flow (GLF)* framework to the double pendulum, a well-known chaotic system. The GLF framework introduces two functions: the truth function Φ and the provability function P, and the difference between these two functions represents the *Gödelian Unpredictability Index (GUI)*.

The double pendulum system is governed by the following set of nonlinear differential equations that describe its motion:

$$\frac{d\theta_1}{dt} = \omega_1$$
$$\frac{d\theta_2}{dt} = \omega_2$$

$$\frac{d\omega_1}{dt} = \frac{-m_2 l_1 \omega_1^2 \sin(\Delta\theta)\cos(\Delta\theta) + m_2 g \sin(\theta_2)\cos(\Delta\theta) + m_2 l_2 \omega_2^2 \sin(\Delta\theta)}{(m_1+m_2)l_1 - m_2 l_1 \cos^2(\Delta\theta)} - \frac{(m_1+m_2)g\sin(\theta_1)}{(m_1+m_2)l_1 - m_2 l_1 \cos^2(\Delta\theta)} \tag{1}$$

$$\frac{d\omega_2}{dt} = \frac{-m_2 l_2 \omega_2^2 \sin(\Delta\theta)\cos(\Delta\theta) + (m_1+m_2)g\sin(\theta_1)\cos(\Delta\theta)}{l_2\left((m_1+m_2)l_1 - m_2 l_1 \cos^2(\Delta\theta)\right)} - \frac{(m_1+m_2)g\sin(\theta_2) + m_2 l_1 \omega_1^2 \sin(\Delta\theta)}{l_2\left((m_1+m_2)l_1 - m_2 l_1 \cos^2(\Delta\theta)\right)} \tag{2}$$

where θ_1 and θ_2 are the angular displacements of the two pendulums, ω_1 and ω_2 are their angular velocities, g is the acceleration due to gravity, m_1 and m_2 are the masses, and l_1 and l_2 are the lengths of the pendulums. $\Delta\theta = \theta_2 - \theta_1$ represents the angular difference between the two pendulums.

The truth function Φ is defined using the system's energy and angular momentum:

$$\Phi(\theta_1, \theta_2, \omega_1, \omega_2) = 1 - \exp(-k_1|L + E|)$$

where L represents the system's angular momentum, and E represents its total energy, calculated as:

$$L = (m_1 + m_2)l_1^2\omega_1 + m_2 l_2^2 \omega_2$$

$$E = \frac{1}{2}(m_1 + m_2)l_1^2\omega_1^2 + \frac{1}{2}m_2 l_2^2\omega_2^2 - (m_1 + m_2)gl_1\cos(\theta_1) - m_2 g l_2 \cos(\theta_2)$$

The provability function P is based on the divergence of angular velocities:

$$P(\theta_1, \theta_2, \omega_1, \omega_2) = 1 - \exp(-k_2|\omega_1 - \omega_2|)$$

The *Gödelian Unpredictability Index (GUI)* is then defined as the magnitude of the difference between the gradients of the truth and provability functions:

$$\text{GUI} = |\nabla\Phi - \nabla P|$$

We also compute the *local Lyapunov exponent* to measure the system's sensitivity to initial conditions, approximating the divergence of nearby trajectories. The Lyapunov exponent is calculated as:

$$\lambda_{\text{Lyap}}(t) = \lim_{t\to 0} \frac{1}{t} \ln\left(\frac{\|DX(t)\cdot v\|}{\|v\|}\right)$$

C.2 Python Implementation

Below is the key Python code used for the double pendulum simulation, incorporating the GLF framework and comparing the GUI to the Lyapunov exponent.

Listing 2: Python code for Double Pendulum and GLF

```
import numpy as np
from scipy.integrate import odeint
import matplotlib.pyplot as plt

# Constants for the double pendulum
g = 9.81  # gravitational acceleration
l1, l2 = 1.0, 1.0  # lengths of the pendulums
m1, m2 = 1.0, 1.0  # masses of the pendulums

# Double pendulum equations of motion
def double_pendulum(state, t):
    theta1, theta2, omega1, omega2 = state
    delta = theta2 - theta1
    denominator1 = (m1 + m2) * l1 - m2 * l1 * np.cos(delta) ** 2
    denominator2 = (l2 / l1) * denominator1
```

```
    dtheta1 = omega1
    dtheta2 = omega2

    domega1 = (m2 * l1 * omega1**2 * np.sin(delta) * np.cos(delta)
               + m2 * g * np.sin(theta2) * np.cos(delta)
               + m2 * l2 * omega2**2 * np.sin(delta)
               - (m1 + m2) * g * np.sin(theta1)) / denominator1

    domega2 = (-m2 * l2 * omega2**2 * np.sin(delta) * np.cos(delta)
               + (m1 + m2) * g * np.sin(theta1) * np.cos(delta)
               - (m1 + m2) * g * np.sin(theta2)
               - m2 * l1 * omega1**2 * np.sin(delta)) / denominator2

    return [dtheta1, dtheta2, domega1, domega2]

# GLF functions
def phi(state, k1):
    L = angular_momentum(state)
    E = total_energy(state)
    return 1 - np.exp(-k1 * abs(L + E))

def p(state, k2):
    theta1, theta2, omega1, omega2 = state
    div = abs(omega1 - omega2)
    return 1 - np.exp(-k2 * div)

# Compute GUI (Godelian Unpredictability Index)
def gui(state, k1, k2):
    return abs(phi(state, k1) - p(state, k2))

# Simulation setup
t = np.linspace(0, 20, 1000)
initial_state = [np.pi / 2, np.pi, 0, 0]
states = odeint(double_pendulum, initial_state, t)

# Detecting and plotting significant events
gui_values = [gui(state, 1, 0.1) for state in states]
lyap_values = [local_lyapunov(state) for state in states]

# Plotting phase space
plt.plot([state[0] for state in states], [state[1] for state in
   states], label="Phase Space Trajectory")
plt.scatter([states[i][0] for i in gui_only_events], [states[i][1]
   for i in gui_only_events], color='r', label="GUI-Only")
plt.scatter([states[i][0] for i in lyap_only_events], [states[i][1]
   for i in lyap_only_events], color='g', label="Lyapunov-Only")
plt.scatter([states[i][0] for i in common_events], [states[i][1] for
    i in common_events], color='b', label="Common Events")
plt.legend()
plt.show()
```

C.3 Results and Discussion

In the double pendulum experiment, we compared the significant events detected by the *Gödelian Unpredictability Index (GUI)* and the *local Lyapunov exponent*. The results demonstrated that the GUI and Lyapunov exponent captured different aspects of the system's behavior. Notably, the GUI detected regions of phase space where logical unpredictability was high due to the system's angular momentum and energy dynamics, while the Lyapunov exponent primarily captured chaotic sensitivity.

The phase space visualization (Figure 1) shows distinct regions of GUI-only events, Lyapunov-only events, and common events. These findings suggest that GUI is sensitive to transitions and resonances in the system that do not necessarily coincide with regions of chaotic sensitivity.

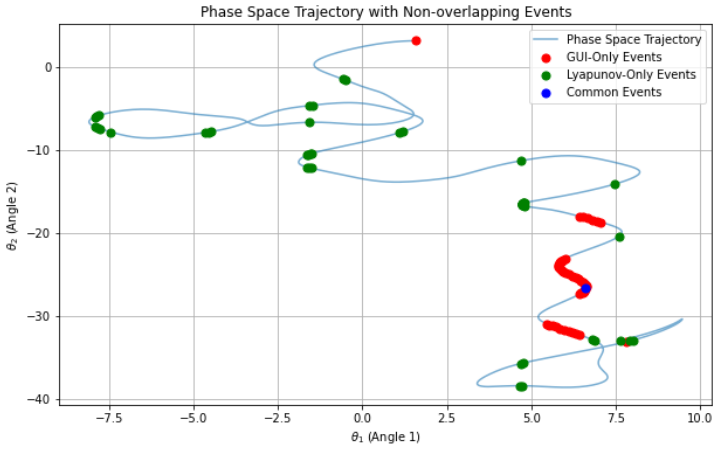

Figure 1: Phase space trajectory of the double pendulum, showing GUI-only, Lyapunov-only, and common significant events.

C.4 Comparing the Double Pendulum and Lorenz System in the GLF Framework

C.4.1 Differences in Chaotic Behavior

The *Lorenz system* and the *double pendulum system* both exhibit chaotic dynamics, but their behavior and the insights provided by the GLF framework are notably different.

C.4.2 Chaotic Sensitivity in the Lorenz System

The Lorenz system is inherently and globally chaotic, meaning that the system exhibits sensitive dependence on initial conditions almost everywhere in its phase space. The equations governing the Lorenz system are given by:

$$\frac{dx}{dt} = \sigma(y - x)$$

$$\frac{dy}{dt} = x(\rho - z) - y$$

$$\frac{dz}{dt} = xy - \beta z$$

where σ, ρ, and β are parameters of the system. In this system, the Lyapunov exponent and the Gödelian Unpredictability Index (GUI) largely align, both detecting chaotic behavior across much of the phase space. The Lorenz system's flow continuously folds and stretches trajectories, leading to a high degree of sensitivity to initial conditions, which is captured effectively by both the GUI and the Lyapunov exponent.

The alignment between the GUI and the Lyapunov exponent in the Lorenz system suggests that this system's chaotic dynamics are highly sensitive to both logical unpredictability (captured by the GUI) and traditional measures of chaos (captured by the Lyapunov exponent). In such systems, chaotic behavior can be viewed as ubiquitous, with no clear separation between logically complex regions and dynamically sensitive regions.

C.4.3 Chaotic Sensitivity in the Double Pendulum

By contrast, the double pendulum system has regions of both chaotic and regular behavior. The motion of the pendulums can be regular and predictable in some parts of the phase space and chaotic in others. This transition between regular and chaotic behavior is an important distinction from the Lorenz system.

The equations of motion for the double pendulum, as discussed in Section 3, include angular velocities ω_1 and ω_2 for each pendulum and are governed by nonlinear forces due to gravity and the pendulum's configuration. The double pendulum's sensitivity to initial conditions varies across its phase space, leading to distinct regions where the Lyapunov exponent and the GUI provide different information.

C.4.4 GLF Differences: Logical Unpredictability vs. Chaotic Sensitivity

One of the key differences between the double pendulum and Lorenz systems in the context of the GLF framework lies in the divergence between the Gödelian Unpredictability Index (GUI) and the Lyapunov exponent in certain regions of the double pendulum's phase space.

C.4.5 Regions of Regular Motion in the Double Pendulum

The double pendulum can exhibit regions of regular, predictable motion, where the system behaves more like a simple pendulum. In these regions, the Lyapunov exponent is low, indicating that the system is not highly sensitive to initial conditions. However, the GUI may still be high in these regions due to the system's internal energy and angular momentum dynamics, which lead to complex interactions that are hard to prove or predict logically.

In essence, the GUI is detecting hidden complexity or unpredictability even in regions where the system does not exhibit traditional chaotic behavior. This complexity may arise from subtle energy exchanges or resonances between the two pendulums, which are not captured by the Lyapunov exponent.

C.4.6 Transition Points and Resonances in the Double Pendulum

Another important feature of the double pendulum system is the existence of **transition points** or **resonances**, where the system shifts from regular to chaotic behavior. These points are of particular interest in the GLF framework because they represent moments

where the system's logical unpredictability (as captured by the GUI) becomes prominent. In these regions, the system may be transitioning between stable, periodic motion and chaotic, sensitive motion.

The GUI captures these transitions as moments of high unpredictability, even though the Lyapunov exponent may not immediately detect the chaotic sensitivity until the system fully transitions into chaos. This difference highlights the value of the GUI in identifying complex dynamics that occur prior to or independent of the system becoming highly sensitive to initial conditions.

C.4.7 Discussion of Results

The results of our simulations confirm the differences between the double pendulum and Lorenz systems. As discussed in Section 4, for the Lorenz system, there was significant overlap between the events detected by the GUI and the Lyapunov exponent, reflecting the system's uniform sensitivity to initial conditions and logical complexity. However, in the double pendulum system, we observed a much smaller overlap between GUI-only and Lyapunov-only events.

The large number of GUI-only events in the double pendulum simulation suggests that the GLF framework is detecting regions of phase space where logical unpredictability is present, even though the system is not yet in a state of chaotic sensitivity. This highlights an important difference between these two systems:

- **In the Lorenz system**, chaotic behavior is pervasive, and the system's sensitive dependence on initial conditions is captured effectively by both the GUI and Lyapunov exponent.
- **In the double pendulum system**, chaotic behavior is more localized, and the GUI detects additional complexity in regions where the system is not immediately sensitive to initial conditions, particularly during transitions or resonances.

C.5 Implications for the GLF Framework

These differences between the Lorenz and double pendulum systems suggest that the GLF framework offers unique insights into the dynamics of chaotic systems. In systems like the Lorenz attractor, where chaotic behavior is dominant, the GUI and Lyapunov exponent provide similar information. However, in systems like the double pendulum, where regular and chaotic behaviors coexist, the GUI can detect complex dynamics that are not captured by traditional chaos measures.

The results of these experiments underscore the value of combining logical complexity (as captured by the GUI) with traditional measures of chaotic sensitivity (like the Lyapunov exponent) to gain a fuller understanding of a system's behavior, particularly in systems with mixed regular and chaotic dynamics.

D GLF Framework for Fluid Dynamics: Mathematical Derivation

In this section, we will formulate the Gödelian-Logical Flow (GLF) framework in the context of a 2D fluid dynamics system. We aim to demonstrate the conceptual alignment

between the GLF framework and chaotic systems, using truth (Φ) and provability (P) as the primary measures.

D.1 Fluid Dynamics: Governing Equations

We begin by considering the vorticity formulation of the Navier-Stokes equations in two dimensions, for an incompressible fluid flow. Let $\omega(x, y, t)$ represent the vorticity, which evolves according to the following equation:

$$\frac{\partial \omega}{\partial t} + \mathbf{u} \cdot \nabla \omega = \nu \nabla^2 \omega$$

where:

- $\mathbf{u} = (u, v)$ is the velocity field,
- ν is the kinematic viscosity,
- $\omega = \frac{\partial v}{\partial x} - \frac{\partial u}{\partial y}$ is the vorticity.

The velocity $\mathbf{u}$ can be recovered from the stream function ψ, which satisfies:

$$\omega = \nabla^2 \psi$$

The velocity components are:

$$u = \frac{\partial \psi}{\partial y}, \quad v = -\frac{\partial \psi}{\partial x}$$

D.2 GLF Functions: Truth (Φ) and Provability (P)

We now introduce the GLF framework by defining two key functions: truth (Φ) and provability (P), which evolve in tandem with the fluid system.

- **Truth Function** ($\Phi(x, y, t)$): This function measures the degree of truth at each point in the fluid. In our setup, we base Φ on the vorticity of the fluid, capturing the chaotic nature of the flow:

  $$\Phi(x, y, t) = 1 - \exp\left(-k_1 \omega^2(x, y, t)\right)$$

  where k_1 is a parameter controlling the sensitivity to vorticity.

- **Provability Function** ($P(x, y, t)$): This function captures the degree of provability, which we relate to the pressure gradient of the system. Specifically, we use the magnitude of the pressure gradient:

  $$P(x, y, t) = 1 - \exp\left(-k_2 |\nabla p(x, y, t)|^2\right)$$

  where $p(x, y, t)$ is the pressure field, and k_2 is a sensitivity parameter.

D.3 GLF Flow: Combining Φ and P

The Gödelian Unpredictability Index (GUI) measures the degree of logical unpredictability, which we define as the difference between truth and provability:

$$\text{GUI}(x, y, t) = \Phi(x, y, t) - P(x, y, t)$$

To evolve the fluid system and the GLF functions over time, we also define the metric evolution using a modified Ricci flow approach:

$$\frac{dg}{dt} = -2\text{Ric}(g) - \nabla\Phi \otimes \nabla\Phi - \nabla P \otimes \nabla P$$

where g is the metric of the system, and $\text{Ric}(g)$ is the Ricci curvature.

D.4 Evolution of the System

To compute the evolution of the system, we use the semi-implicit time-stepping method to update the vorticity ω, stream function ψ, and pressure gradient ∇p. The nonlinear advection term is computed from the velocity field $\mathbf{u}$, and the system evolves according to the Navier-Stokes equations:

$$\frac{\partial \omega}{\partial t} = -\mathbf{u} \cdot \nabla\omega + \nu\nabla^2\omega$$

The GLF metrics Φ, P, and GUI are updated at each timestep based on the current vorticity and pressure gradient.

D.5 Key Equations Summary

The full set of equations governing the system is summarized as follows:

1. Vorticity evolution:
$$\frac{\partial \omega}{\partial t} = -\mathbf{u} \cdot \nabla\omega + \nu\nabla^2\omega$$
2. Truth Function:
$$\Phi(x, y, t) = 1 - \exp\left(-k_1\omega^2(x, y, t)\right)$$
3. Provability Function:
$$P(x, y, t) = 1 - \exp\left(-k_2|\nabla p(x, y, t)|^2\right)$$
4. Gödelian Unpredictability Index (GUI):
$$\text{GUI}(x, y, t) = \Phi(x, y, t) - P(x, y, t)$$

D.6 Fluid Dynamics Setup and Simulation

In this simulation, we use a 2D grid to simulate the evolution of the fluid and GLF functions. The key steps in the simulation are as follows:

D.6.1 Grid Initialization

The fluid is initialized on a 2D periodic grid with random perturbations in the vorticity field. We define the stream function ψ and compute the velocity field $\mathbf{u}$ using Fourier transforms.

D.6.2 Time Stepping

- The vorticity ω evolves according to the Navier-Stokes equations with advection and dissipation.
- The GLF functions Φ, P, and GUI are updated at each timestep using the current vorticity and pressure gradient.
- We compute the Lyapunov exponent for the system to compare with the GLF measures.

D.6.3 Analysis

At each timestep, we record the mean values of Φ, P, and GUI, as well as the Lyapunov exponent. We normalize and compare the evolution of these metrics to study their correlation.

D.6.4 Results and Discussion

In Figure 2, we show the evolution of the normalized Lyapunov exponent, G, and GUI over time. Initially, both the Lyapunov exponent and GUI exhibit high values, indicating the chaotic and unpredictable nature of the fluid system in its early, turbulent phase.

However, as the system evolves, the Lyapunov exponent and GUI begin to behave differently. The Lyapunov exponent spikes early, indicating a burst of chaotic behavior, followed by a rapid decline as the system stabilizes. On the other hand, the GUI also starts high but declines more gradually, reflecting the system's transition from being logically unpredictable to becoming more "provable" in the GLF sense.

D.6.5 Statistical Analysis and Dynamical Behavior

While the statistical correlation between the Lyapunov exponent and GUI is negative (-0.79), this number alone does not capture the full complexity of the system's dynamics. Both measures start high during the turbulent phase, but GUI drops more slowly, potentially indicating that the logical structure of the system continues to exhibit complexity even as the chaos subsides.

Table 1: Key Statistics between Lyapunov Exponent and GLF Terms

Metric	**Lyapunov vs. G**	**Lyapunov vs. GUI**
Correlation	-0.65	-0.79
Sign Agreement (%)	99.00%	99.00%
Standard Deviation (Lyapunov)	0.12	0.12
Standard Deviation (GLF Term)	0.37 (G)	0.33 (GUI)

D.7 Discussion

The fluid system undergoes a transition from chaotic, turbulent flow to a more stable, laminar state. Initially, the Lyapunov exponent spikes due to chaotic behavior, while the GUI remains high, suggesting that both measures capture the system's instability. However, the GUI's gradual decline, compared to the sharper drop in the Lyapunov exponent, suggests that the GLF framework captures aspects of logical unpredictability that persist even as the chaos diminishes.

This divergence in behavior emphasizes that while both GUI and the Lyapunov exponent measure aspects of unpredictability, they may be capturing different types of complexity. The GLF framework might be sensitive to features of the system that reflect the provability or logical structure, not just sensitivity to initial conditions.

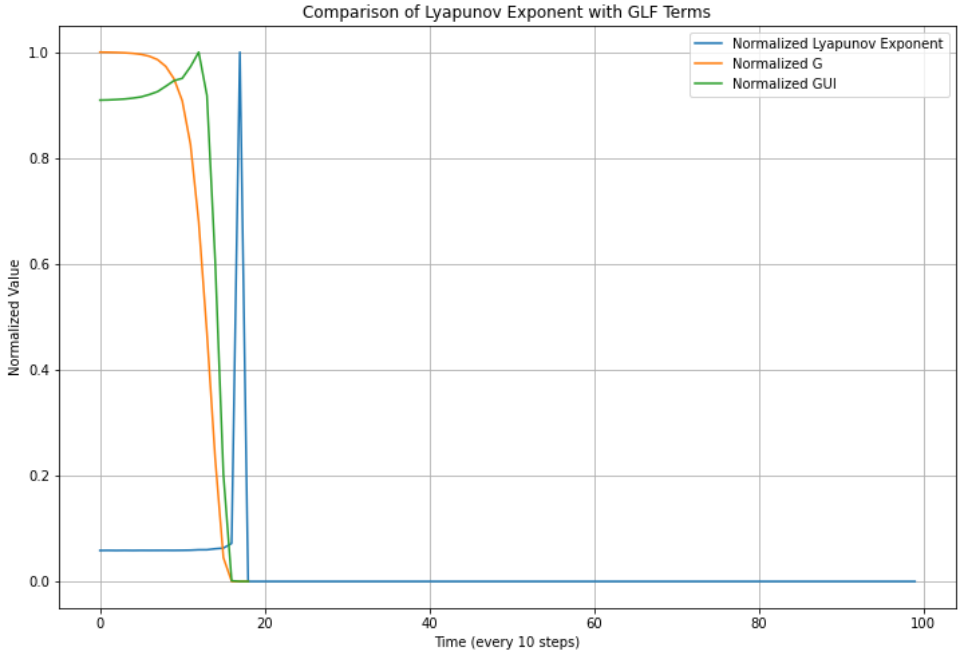

Figure 2: Evolution of the GLF framework (GUI, Φ, P) compared with the Lyapunov exponent in fluid flow.

D.8 Python code for Fluid Flow Model

Listing 3: Key Python Code for GLF and Lyapunov Comparison in Fluid Dynamics

```
import numpy as np
import matplotlib.pyplot as plt
from scipy.fftpack import fft2, ifft2, fftfreq
import scipy.stats as stats

# Simulation parameters
N = 128  # Number of grid points in each direction
L = 2 * np.pi  # Domain size
```

```
dt = 0.01  # Time step
nt = 1000  # Number of time steps
nu = 1e-3  # Kinematic viscosity

# GLF parameters
G0 = 1.0
k1 = 0.1
k2 = 0.1
alpha = 0.1
beta = 0.1
gamma = 2.0

# Initialize grid and wavenumbers
x = np.linspace(0, L, N, endpoint=False)
y = np.linspace(0, L, N, endpoint=False)
X, Y = np.meshgrid(x, y)
kx = fftfreq(N, L / N)
ky = fftfreq(N, L / N)
KX, KY = np.meshgrid(kx, ky)
K2 = KX ** 2 + KY ** 2
K2[0, 0] = 1  # Avoid division by zero

# Initialize vorticity
omega = np.sin(X) * np.cos(Y) + 0.1 * np.random.randn(N, N)

# Functions for computation of stream function, velocity,
    pressure gradient
def compute_stream_function(omega):
    return ifft2(-fft2(omega) / K2).real

def compute_velocity(psi):
    u = ifft2(1j * KY * fft2(psi)).real
    v = ifft2(-1j * KX * fft2(psi)).real
    return u, v

def compute_pressure_gradient(u, v):
    ux = ifft2(1j * KX * fft2(u)).real
    uy = ifft2(1j * KY * fft2(u)).real
    vx = ifft2(1j * KX * fft2(v)).real
    vy = ifft2(1j * KY * fft2(v)).real
    p = ifft2(-(KX ** 2 * fft2(u * u) + 2 * KX * KY * fft2(u * v
        ) + KY ** 2 * fft2(v * v)) / K2).real
    return ifft2(1j * KX * fft2(p)).real, ifft2(1j * KY * fft2(p
        )).real

# Compute G based on omega and pressure gradient
def compute_G(omega, grad_p):
    omega_squared = np.clip(omega ** 2, 0, 1e10)  # Clip to
```

```
        prevent overflow
    grad_p_squared = np.clip(grad_p[0] ** 2 + grad_p[1] ** 2, 0,
        1e10)
    exponent = -k1 * (np.mean(omega_squared) + np.mean(
        grad_p_squared))
    return G0 * np.exp(np.clip(exponent, -100, 100))  # Clip
        exponent to prevent underflow/overflow

# Compute GUI based on G, omega, and pressure gradient
def compute_GUI(G, omega, grad_p):
    vorticity_term = alpha * np.tanh(G) * np.log1p(np.abs(omega)
        )
    pressure_magnitude = np.clip(np.sqrt(grad_p[0] ** 2 + grad_p
        [1] ** 2), 0, 1e10)
    pressure_term = beta * np.tanh(G) * np.power(1 +
        pressure_magnitude, gamma)
    return vorticity_term + pressure_term

# Evolution of the system
def evolve(omega):
    psi = compute_stream_function(omega)
    u, v = compute_velocity(psi)
    grad_p = compute_pressure_gradient(u, v)
    G = compute_G(omega, grad_p)
    GUI = compute_GUI(G, omega, grad_p)
    N = compute_nonlinear(psi, omega)

    omega_hat = fft2(omega)
    N_hat = fft2(N)
    GUI_hat = fft2(GUI)

    omega_new_hat = (omega_hat + dt * (N_hat + 1j * (KX *
        GUI_hat * G + KY * GUI_hat * G))) / (1 + nu * dt * K2)
    omega_new = ifft2(omega_new_hat).real

    return omega_new, G, np.mean(GUI)

# Compute Lyapunov exponent
def compute_lyapunov(omega, n_iterations=10):
    perturbation = 1e-5 * np.random.randn(*omega.shape)
    omega_perturbed = omega + perturbation
    lyap_sum = 0

    for _ in range(n_iterations):
        omega, _, _ = evolve(omega)
        omega_perturbed, _, _ = evolve(omega_perturbed)

        new_perturbation = omega_perturbed - omega
```

```
        d = np.linalg.norm(new_perturbation)
        if d > 1e-10:  # Avoid log(0)
            lyap_sum += np.log(d / 1e-5)

        if d > 1e-10:
            omega_perturbed = omega + 1e-5 * new_perturbation /
                d
        else:
            omega_perturbed = omega + 1e-5 * np.random.randn(*
                omega.shape)

    return lyap_sum / (n_iterations * dt)

# Normalization and plotting
def safe_normalize(x):
    x_min, x_max = np.nanmin(x), np.nanmax(x)
    if x_max > x_min:
        return (x - x_min) / (x_max - x_min)
    else:
        return np.zeros_like(x)

# Main simulation loop and data collection
omega_history = []
lyap_history = []
g_history = []
gui_history = []

for n in range(nt):
    omega, G, GUI = evolve(omega)

    if n % 10 == 0:
        omega_history.append(omega)
        lyap = compute_lyapunov(omega)
        lyap_history.append(lyap)
        g_history.append(G)
        gui_history.append(GUI)

# Normalize and plot results
lyap_norm = safe_normalize(lyap_history)
g_norm = safe_normalize(g_history)
gui_norm = safe_normalize(gui_history)

plt.figure(figsize=(12, 8))
plt.plot(lyap_norm, label='Normalized Lyapunov Exponent')
plt.plot(g_norm, label='Normalized G')
plt.plot(gui_norm, label='Normalized GUI')
plt.xlabel('Time (every 10 steps)')
plt.ylabel('Normalized Value')
```

```
plt.title('Comparison of Lyapunov Exponent with GLF Terms')
plt.legend()
plt.grid(True)
plt.show()
```

E Gödelian Unpredictability in Hyperion's Chaotic Rotation

E.1 Mathematical Derivation of the Gödelian Unpredictability Index (GUI)

In this section, we derive the application of the Gödelian-Logical Flow (GLF) framework to Hyperion's chaotic rotation. The Gödelian Unpredictability Index (GUI) is central to this analysis, aiming to capture logical unpredictability through a rigorous mathematical formulation derived from the GLF principles.

Hyperion's chaotic rotation is governed by the Euler equations for rigid body dynamics:

$$\frac{d\omega_1}{dt} = I_2\omega_2\omega_3 - I_3\omega_2\omega_3, \quad \frac{d\omega_2}{dt} = I_3\omega_3\omega_1 - I_1\omega_3\omega_1, \quad \frac{d\omega_3}{dt} = I_1\omega_1\omega_2 - I_2\omega_1\omega_2 \tag{3}$$

where $\omega_1, \omega_2, \omega_3$ are the angular velocities, and I_1, I_2, I_3 are the moments of inertia. These equations describe the non-linear interactions between the angular velocities and reveal the system's susceptibility to chaotic behavior, particularly as it responds to perturbations over time.

The Gödelian Unpredictability Index (GUI) is formulated based on two core concepts: truth and provability in the system. To represent these within a physical system like Hyperion, we define the following:

- Truth function $\Phi(\omega)$: Related to the rotational kinetic energy (KE), capturing the fundamental "truth" of the system's energetic state:

$$\Phi(\omega) = 1 - e^{-k_1 \cdot KE(\omega)}, \quad KE(\omega) = \frac{1}{2}(I_1\omega_1^2 + I_2\omega_2^2 + I_3\omega_3^2)$$

The exponential form ensures that the truth function approaches 1 as kinetic energy increases, reflecting that high-energy states are highly deterministic in their truth.

- Provability function $P(\omega)$: Linked to the divergence of the angular velocities, reflecting the system's capacity for predictable and provable outcomes:

$$P(\omega) = 1 - e^{-k_2 \cdot |\nabla \cdot \omega|}$$

This function decreases with increasing divergence, reflecting the system's loss of provability as the angular velocities become more misaligned.

The GUI is defined as the magnitude of the difference between the gradients of Φ and P, quantifying the local unpredictability:

$$GUI(\omega) = \|\nabla\Phi(\omega) - \nabla P(\omega)\|$$

This expression captures the discrepancy between what is logically true (kinetically determinable) and what can be predicted or proven (based on angular velocity alignment).

The GUI thus integrates both physical and logical elements of unpredictability, distinguishing it from classical chaos measures such as the Lyapunov exponent, which purely tracks the divergence of trajectories in phase space.

E.2 Methodology

1. Simulation Setup: We simulate the rotational dynamics of Hyperion using numerical integration of the Euler equations. The system is initialized with small perturbations in the angular velocities $\omega_1, \omega_2, \omega_3$, and integrated over time. The evolution of the system is tracked over a long time horizon to capture chaotic transitions.

2. Computation of GUI: At each time step, the rotational kinetic energy and the divergence of angular velocities are computed to evaluate $\Phi(\omega)$ and $P(\omega)$, respectively. The GUI is computed as the norm of the difference between the gradients of these two functions.

3. Lyapunov Exponent Calculation: The Lyapunov exponent is computed using a finite-difference method, tracking the rate of separation of initially close trajectories. This provides a baseline measure of classical chaos for comparison with the GUI.

E.3 Results

The following table summarizes the correlation between the GUI and key physical parameters, including kinetic energy and angular velocities:

Parameter	**Correlation with GUI**
Kinetic Energy	0.7846
Angular Velocity ω_1	0.3996
Angular Velocity ω_2	-0.0259
Angular Velocity ω_3	-0.0400

Table 2: Correlation between GUI and various physical parameters in Hyperion's rotation.

The figures below illustrate the evolution of the GUI, Lyapunov exponent, kinetic energy, and angular velocities over time.

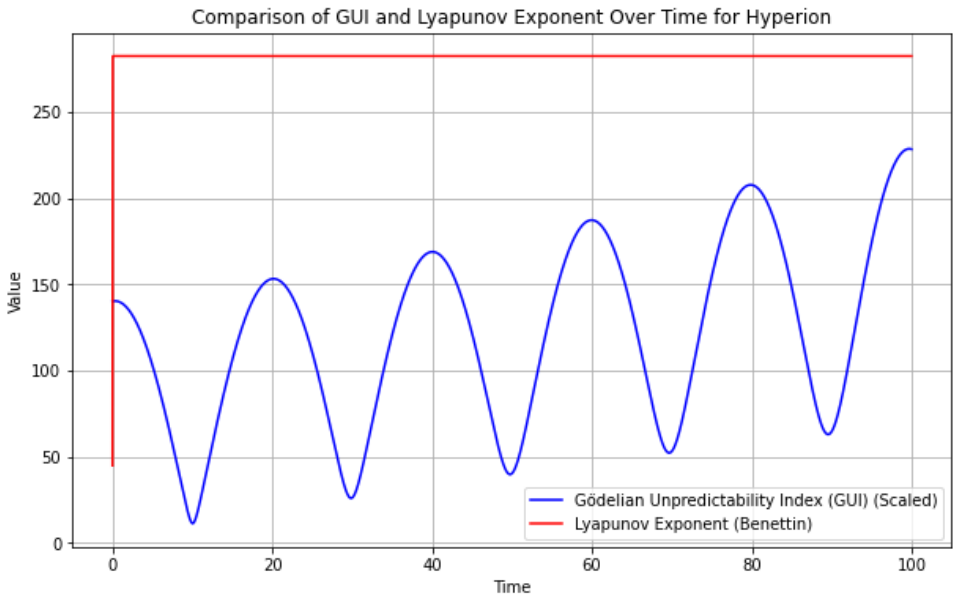

Figure 3: Comparison of the GUI and Lyapunov Exponent (Benettin) over time.

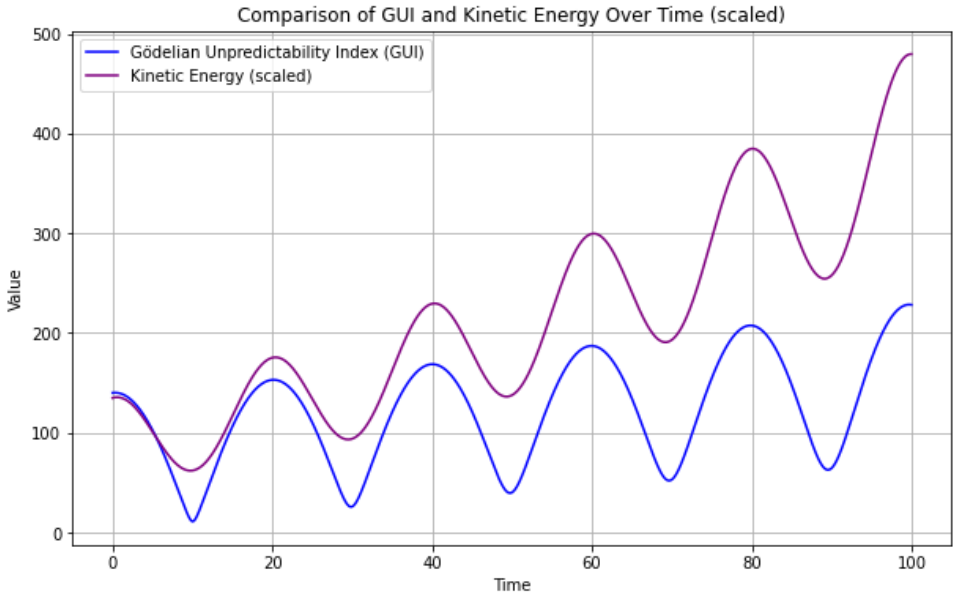

Figure 4: Comparison of the GUI and kinetic energy over time.

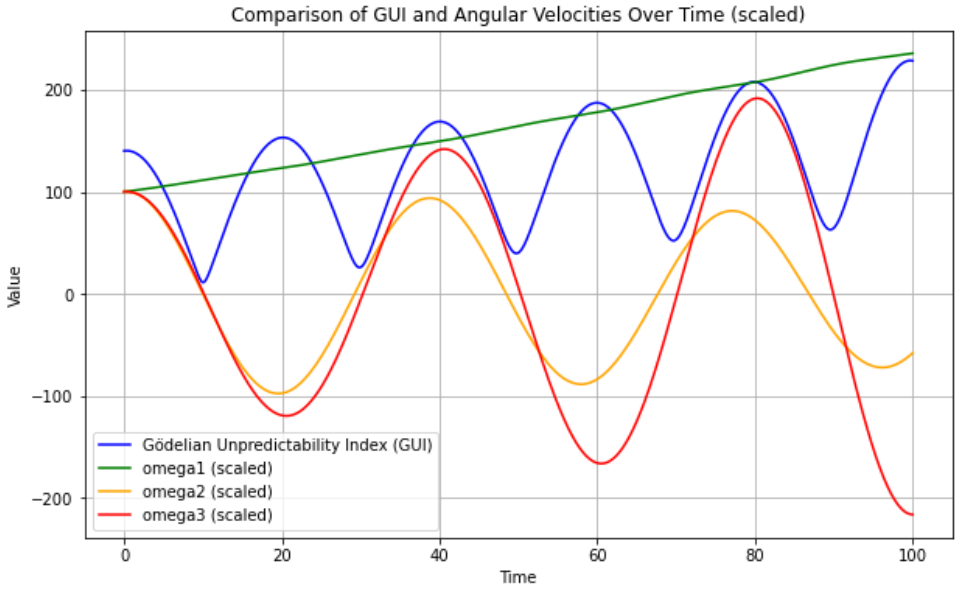

Figure 5: Comparison of the GUI and angular velocities over time.

E.4 Discussion

The results indicate a strong correlation between the Gödelian Unpredictability Index (GUI) and kinetic energy, with a coefficient of 0.7846. This suggests that the system's logical unpredictability, as captured by the GUI, is closely tied to its energy dynamics. In contrast, the angular velocities ω_2 and ω_3 showed weak negative correlations with the GUI, implying that these variables contribute less to logical unpredictability compared to kinetic energy.

E.4.1 Relation to Other Chaotic Systems

The behavior of the GUI in Hyperion's rotation is consistent with patterns observed in other chaotic systems, such as the double pendulum and the Lorenz attractor, where logical unpredictability tends to rise with increasing system energy. However, unlike those systems, Hyperion exhibits periodic fluctuations in the GUI despite maintaining a steady Lyapunov exponent. This suggests that physical chaos and logical unpredictability evolve differently in this system.

E.4.2 Interpretation of GUI vs. Lyapunov Exponent

The Lyapunov exponent measures the rate of divergence of nearby trajectories, capturing physical sensitivity to initial conditions. However, the GUI extends beyond this by incorporating logical flow—capturing discrepancies between what is true (based on the system's energy) and what can be proven or predicted. This distinction is particularly relevant in regions of chaotic systems where energy fluctuations drive complex behavior, even when the overall system remains physically chaotic.

The strong correlation between the GUI and kinetic energy suggests that the system's unpredictability in logical terms grows as the total energy increases. This highlights the fundamental role energy plays, not only in driving physical chaos but also in determining the system's provability and logical complexity.

E.4.3 Different Forms of Unpredictability

The analysis reveals that chaotic systems can exhibit different forms of unpredictability. The GUI highlights a form of logical unpredictability that is distinct from the physical chaos measured by the Lyapunov exponent. This distinction suggests that chaotic systems operate at multiple levels of unpredictability—physical and logical—each contributing uniquely to the system's overall behavior.

E.4.4 Meaning of GUI: Provability vs. Truth

The GUI captures the gap between truth (as determined by energy dynamics) and provability (as determined by angular velocity divergence). This idea aligns with Gödelian principles, where not all truths in a system can be proven, particularly as the system becomes more complex. In Hyperion's case, as energy increases, the divergence between provability and truth widens, reflecting the growing complexity of the system's dynamics.

E.4.5 Implications for Quantum-Classical Correspondence

The behavior of Hyperion's chaotic rotation raises important questions about the quantum-classical correspondence, particularly beyond the Ehrenfest time, where classical systems begin to diverge from quantum mechanical predictions. As discussed by Zurek (1998), chaos and decoherence create challenges for this correspondence. The GUI provides a new perspective on this issue, suggesting that the logical complexity of a system could play a role in why certain chaotic systems resist quantum predictability, even under classical conditions.

E.4.6 Conclusion

In summary, the GUI offers a deeper understanding of unpredictability in chaotic systems by integrating physical chaos and logical complexity. This framework has broad implications for both classical and quantum dynamics, offering a valuable tool to explore the limits of predictability in highly chaotic environments.

E.5 Python Code for GUI and Lyapunov Exponent Computation

Listing 4: Python code for Hyperion's chaotic rotation

```
import numpy as np
from scipy.integrate import solve_ivp
import matplotlib.pyplot as plt
from scipy.stats import pearsonr

# Constants for Hyperion's chaotic rotation
I1, I2, I3 = 1.0, 0.9, 0.8  # Principal moments of inertia
n = 0.1  # Mean motion (orbital angular velocity)

# Define the system of differential equations for Hyperion's
    rotation
def hyperion_rotation(t, state):
    omega1, omega2, omega3, gamma1, gamma2, gamma3 = state
    d_omega1 = I1 * (omega2 * omega3 - 3 * n**2 * gamma2 * gamma3)
    d_omega2 = I2 * (omega3 * omega1 + 3 * n**2 * gamma1 * gamma3)
    d_omega3 = I3 * (omega1 * omega2 - 3 * n**2 * gamma1 * gamma2)
    d_gamma1 = omega2 * gamma3 - omega3 * gamma2
    d_gamma2 = omega3 * gamma1 - omega1 * gamma3
    d_gamma3 = omega1 * gamma2 - omega2 * gamma1
    return [d_omega1, d_omega2, d_omega3, d_gamma1, d_gamma2,
        d_gamma3]

# Define the truth function Phi (related to rotational kinetic
    energy)
def phi(state, k1):
    omega1, omega2, omega3, *_ = state
    KE = 0.5 * (I1 * np.clip(omega1, -10, 10)**2 + I2 * np.clip(
        omega2, -10, 10)**2 + I3 * np.clip(omega3, -10, 10)**2)
    return 1 - np.exp(-k1 * KE)

# Define the provability function P (related to angular velocity
    alignment)
def p(state, k2):
    omega1, omega2, omega3, gamma1, gamma2, gamma3 = state
    alignment = np.abs(np.cross([omega1, omega2, omega3], [gamma1,
        gamma2, gamma3]))
    alignment_norm = np.linalg.norm(np.clip(alignment, -10, 10))
    return 1 - np.exp(-k2 * alignment_norm)
```

```
# Define the G delian Unpredictability Index (GUI)
def gui(state, k1, k2):
    grad_phi = phi(state, k1)
    grad_p = p(state, k2)
    return np.abs(grad_phi - grad_p)

# Function to compute Lyapunov exponent using Benettin's algorithm
def benettin_lyapunov(f, initial_state, t, delta=1e-6):
    initial_state = np.array(initial_state)
    perturbed_state = initial_state + delta  # Perturbation in the
        initial condition
    lyapunov_exp = []  # List to store Lyapunov exponent values over
        time

    # Iterate over time steps (use len(t) - 1 to avoid out-of-bounds
        )
    for i in range(len(t) - 1):
        # Solve the system for both the original and perturbed
            states over the current time interval
        sol1 = solve_ivp(f, [t[i], t[i + 1]], initial_state, method=
            'RK45')
        sol2 = solve_ivp(f, [t[i], t[i + 1]], perturbed_state,
            method='RK45')

        # Calculate the distance between the original and perturbed
            solutions
        dist = np.linalg.norm(sol1.y[:, -1] - sol2.y[:, -1])

        # Normalize the perturbed state to keep it close to the
            original
        perturbed_state = sol1.y[:, -1] + delta * (sol2.y[:, -1] -
            sol1.y[:, -1]) / dist

        # Update Lyapunov exponent for this time step
        lyapunov_exp.append(np.log(dist / delta))

    return np.array(lyapunov_exp) / (t[1] - t[0])  # Normalize by
        time interval

# Initial conditions
initial_state = [0.01, 0.01, 0.01, 1.0, 0.0, 0.0]

# Time points (extended to 100 time units)
t = np.linspace(0, 100, 5000)

# Scaling parameters for GUI
k1, k2 = 0.01, 0.01

# Solve the system for the original initial conditions
sol = solve_ivp(hyperion_rotation, [0, 100], initial_state, t_eval=t
    , method='RK45')
```

```
# Calculate the GUI over time
gui_values = np.array([gui(state, k1, k2) for state in sol.y.T])

# Calculate the Lyapunov exponent over time using Benettin's
    algorithm
lyap_exp_values = benettin_lyapunov(hyperion_rotation, initial_state
    , t)

# Angular velocities
omega1, omega2, omega3 = sol.y[0], sol.y[1], sol.y[2]

# Calculate kinetic energy over time
KE_values = 0.5 * (I1 * omega1**2 + I2 * omega2**2 + I3 * omega3**2)

# Scale values for better comparison
scaled_KE = KE_values * 1e6  # Scale kinetic energy by 1e6
scaled_omega1 = omega1 * 1e4  # Scale omega1 by 1e4
scaled_omega2 = omega2 * 1e4  # Scale omega2 by 1e4
scaled_omega3 = omega3 * 1e4  # Scale omega3 by 1e4

# Plot GUI vs KE and angular velocities with scaling
plt.figure(figsize=(10, 6))
plt.plot(t, gui_values * 1e6, label="Godelian Unpredictability Index
    (GUI)", color='blue')
plt.plot(t, scaled_KE, label="Kinetic Energy (scaled)", color='
    purple')
plt.xlabel('Time')
plt.ylabel('Value')
plt.title('Comparison of GUI and Kinetic Energy Over Time (scaled)')
plt.legend()
plt.grid(True)
plt.show()

plt.figure(figsize=(10, 6))
plt.plot(t, gui_values * 1e6, label="Godelian Unpredictability Index
    (GUI)", color='blue')
plt.plot(t, scaled_omega1, label="omega1 (scaled)", color='green')
plt.plot(t, scaled_omega2, label="omega2 (scaled)", color='orange')
plt.plot(t, scaled_omega3, label="omega3 (scaled)", color='red')
plt.xlabel('Time')
plt.ylabel('Value')
plt.title('Comparison of GUI and Angular Velocities Over Time (
    scaled)')
plt.legend()
plt.grid(True)
plt.show()

# Correlation calculations between GUI and KE, omega1, omega2,
    omega3
correlation_gui_ke, _ = pearsonr(gui_values, KE_values)
```

```
correlation_gui_omega1, _ = pearsonr(gui_values, omega1)
correlation_gui_omega2, _ = pearsonr(gui_values, omega2)
correlation_gui_omega3, _ = pearsonr(gui_values, omega3)

# Output correlation results
print(f"Correlation between GUI and Kinetic Energy: {
    correlation_gui_ke}")
print(f"Correlation between GUI and omega1: {correlation_gui_omega1}
    ")
print(f"Correlation between GUI and omega2: {correlation_gui_omega2}
    ")
print(f"Correlation between GUI and omega3: {correlation_gui_omega3}
    ")
```

F Appendix: Mathematical Summary

F.1 Part 1: Core Definitions

Gödelian-Topos Manifold: Definition 1.1: A Gödelian-Topos Manifold is a tuple (M, g, Φ, P) where:

- M is a smooth n-dimensional manifold.
- g is a Riemannian metric on M.
- $\Phi, P : M \to [0, 1]$ are smooth functions satisfying $P \leq \Phi$ pointwise.

Gödelian Ricci Flow: Definition 2.1: A Gödelian Ricci Flow is a one-parameter family $(g(t), \Phi(t), P(t))$ satisfying:

$$\frac{\partial g}{\partial t} = -2Ric(g) - \nabla\Phi \otimes \nabla\Phi - \nabla P \otimes \nabla P$$

$$\frac{\partial \Phi}{\partial t} = \Delta_g \Phi + |\nabla \Phi|_g^2$$

$$\frac{\partial P}{\partial t} = \Delta_g P + (\Phi - P)$$

Discrete Gödelian Space: Definition 2.1: A Discrete Gödelian Space is a triple (X, Φ_X, P_X) where:

- X is an object in a discrete category E.
- $\Phi_X, P_X : X \to \Omega_G$ are morphisms satisfying consistency and Gödelian property conditions.

Gödelian Unpredictability Index (GUI):

$$GUI(x) = \lim_{r \to 0} \left(\frac{1}{V(B_r(x))} \right) \int_{B_r(x)} (\Phi(y) - P(y)) dV_g(y)$$

where $B_r(x)$ is the ball of radius r centered at x, and $V(B_r(x))$ is its volume.

Gödelian Fractal Dimension (GFD):

$$GFD(A) = \lim_{\epsilon \to 0} \frac{\log(N_G(\epsilon))}{\log(1/\epsilon)}$$

where $N_G(\epsilon)$ is the minimum number of ϵ-balls needed to cover A, measured using the metric:

$$d_G(x, y) = \left(\int_\gamma e^{(\Phi + P)} ds \right)^{1/2}$$

where γ is the geodesic from x to y.

F.2 Part 2: Theorems and Lemmas

Gödelian Index Theorem: Theorem 3.3: For a Gödelian elliptic differential operator D on a compact Gödelian-Topos Manifold (M, g, Φ, P):

$$ind_G(D) = \int_M \hat{A}_G(M)\, ch_G(\sigma(D))\, Todd_G(TM \otimes \mathbb{C})$$

Gödelian Weyl Law: Theorem 9.2:

$$N_G(\lambda) \sim \frac{Vol_G(M)}{(4\pi)^{n/2}\Gamma(n/2+1)} \lambda^{n/2} \quad \text{as } \lambda \to \infty$$

Discrete Gödelian Index: Definition 3.2: For a Discrete Gödelian Operator T on a finite Discrete Gödelian Space X:

$$Ind_G(T) = \dim(\ker(T)) - \dim(\text{coker}(T)) + \int_X (\Phi_X - P_X) d\mu$$

Discrete Gödelian Index Theorem: Theorem 3.3: For a finite Discrete Gödelian Space (X, Φ_X, P_X) and Discrete Gödelian Operator T:

$$Ind_G(T) = \sum_{x \in X} (\Phi_X(x) - P_X(x)) \cdot \chi(Fix(T, x))$$

Discrete Gödelian Ricci Flow: Definition 5.1: For a time-dependent Gödelian graph $G(t) = (V, E(t), \Phi(t), P(t))$:

$$\frac{d}{dt} w_{ij}(t) = -2Ric_{ij}(t) - \nabla_i \Phi(t) \nabla_j \Phi(t) - \nabla_i P(t) \nabla_j P(t)$$

$$\frac{d}{dt} \Phi_i(t) = \Delta_G \Phi_i(t) + |\nabla \Phi_i(t)|^2$$

$$\frac{d}{dt} P_i(t) = \Delta_G P_i(t) + (\Phi_i(t) - P_i(t))$$

Undecidability of Gödelian Halting: Theorem 8.5: The problem of determining whether $\Phi_M(x) > P_M(x)$ for arbitrary M and x is undecidable.

Approximation Complexity of Gödelian Index: Theorem 8.6: For any $\epsilon > 0$, approximating Ind_G to within ϵ for general Discrete Gödelian Spaces is #P-hard.

FPRAS for Planar Gödelian Graphs: Theorem 8.7: There exists a fully polynomial randomized approximation scheme (FPRAS) for computing Ind_G of planar Gödelian graphs.

F.3 Part 3: Chaotic Systems Formulations

Lorenz System: Equations of motion:

$$\frac{dx}{dt} = \sigma(y - x), \quad \frac{dy}{dt} = x(\rho - z) - y, \quad \frac{dz}{dt} = xy - \beta z$$

GLF functions:

$$\Phi(x, y, z) = 1 - \exp(-k_1(x^2 + y^2 + z^2)), \quad P(x, y, z) = 1 - \exp(-k_2|\nabla \cdot f(x, y, z)|)$$

where f represents the Lorenz vector field, and k_1, k_2 are constants.

Double Pendulum: Equations of motion:

$$\frac{d\theta_1}{dt} = \omega_1, \quad \frac{d\theta_2}{dt} = \omega_2$$

$$\frac{d\omega_1}{dt} = \frac{-m_2 l_1 \omega_1^2 \sin(\Delta\theta)\cos(\Delta\theta) + m_2 g \sin(\theta_2)\cos(\Delta\theta) + m_2 l_2 \omega_2^2 \sin(\Delta\theta) - (m_1 + m_2) g \sin(\theta_1)}{(m_1 + m_2) l_1 - m_2 l_1 \cos^2(\Delta\theta)}$$

$$\frac{d\omega_2}{dt} = \frac{-m_2 l_2 \omega_2^2 \sin(\Delta\theta)\cos(\Delta\theta) + (m_1 + m_2) g \sin(\theta_1)\cos(\Delta\theta) - (m_1 + m_2) g \sin(\theta_2) + m_2 l_1 \omega_1^2 \sin(\Delta\theta)}{l_2((m_1 + m_2) l_1 - m_2 l_1 \cos^2(\Delta\theta))}$$

where $\Delta\theta = \theta_2 - \theta_1$.

GLF functions:

$$\Phi(\theta_1, \theta_2, \omega_1, \omega_2) = 1 - \exp(-k_1|L + E|), \quad P(\theta_1, \theta_2, \omega_1, \omega_2) = 1 - \exp(-k_2|\omega_1 - \omega_2|)$$

where L is angular momentum, E is total energy, and k_1, k_2 are constants.

Fluid Dynamics (2D vorticity formulation): Equation of motion:

$$\frac{\partial \omega}{\partial t} + u \cdot \nabla \omega = \nu \nabla^2 \omega$$

where ω is vorticity, u is velocity, and ν is kinematic viscosity.

GLF functions:

$$\Phi(x, y, t) = 1 - \exp(-k_1 \omega^2(x, y, t)), \quad P(x, y, t) = 1 - \exp(-k_2|\nabla p(x, y, t)|^2)$$

where p is pressure, and k_1, k_2 are constants.

F.4 Part 4: Hyperion's Chaotic Rotation and Additional Formulas

Hyperion's Chaotic Rotation: Equations of motion (Euler equations):

$$\frac{d\omega_1}{dt} = I_2 \omega_2 \omega_3 - I_3 \omega_2 \omega_3, \quad \frac{d\omega_2}{dt} = I_3 \omega_3 \omega_1 - I_1 \omega_3 \omega_1, \quad \frac{d\omega_3}{dt} = I_1 \omega_1 \omega_2 - I_2 \omega_1 \omega_2$$

where $\omega_1, \omega_2, \omega_3$ are angular velocities, and I_1, I_2, I_3 are moments of inertia.

GLF functions:

$$\Phi(\omega) = 1 - \exp(-k_1 \cdot KE(\omega)), \quad P(\omega) = 1 - \exp(-k_2 \cdot |\nabla \cdot \omega|)$$

where $KE(\omega) = \frac{1}{2}(I_1 \omega_1^2 + I_2 \omega_2^2 + I_3 \omega_3^2)$ is the rotational kinetic energy.

Additional Key Formulas:

- **Gödelian Unpredictability Index (GUI):**

$$GUI(\omega) = ||\nabla\Phi(\omega) - \nabla P(\omega)||$$

- **Local Lyapunov Exponent:**

$$\lambda_{GLF}(x) = \lim_{t\to 0} \frac{1}{t} \ln\left(\frac{||DX(x)\cdot v||}{||v||}\right)$$

  where $DX(x)$ is the Jacobian of X at x, and v is a tangent vector.

- **GLF Entropy:**

$$h_{GLF} = \lim_{T\to\infty} \frac{1}{T} \ln\left(\int_M \exp\left(\int_0^T GUI(\varphi_t(x))dt\right) dx\right)$$

  where φ_t is the flow generated by X.

- **GLF-Chaos Measure:**

$$\Psi(x,t) = GUI(x) \cdot \exp\left(\int_0^t \lambda_{GLF}(\varphi_s(x))ds\right)$$

- **Gödelian Entropy Functional:**

$$S_G(g,\Phi,P) = \int_M \left(R_g + |\nabla\Phi|^2 + |\nabla P|^2 + (\Phi - P)^2\right) e^{-(\Phi+P)} dV_g$$

  where R_g is the scalar curvature of the metric g.

Conjectures:

- **GLF-Chaos Correspondence Principle:** For a large class of systems, there exists a choice of Φ and P such that:

$$\lim_{t\to\infty} \frac{1}{t} \ln(\Psi(x,t)) = \lambda$$

  where λ is the largest Lyapunov exponent of the system in the classical sense.

This appendix provides a comprehensive summary of the key mathematical definitions, theorems, lemmas, and formulas presented in the paper, offering a quick reference for the core concepts of the Gödelian-Logical Flow framework and its application to various chaotic systems.

References

[1] Alam, S., Ata, M., Bailey, S., *et al.* (2017). The Completed SDSS-IV extended Baryon Oscillation Spectroscopic Survey: Cosmological Implications from Two Decades of Spectroscopic Surveys at the Apache Point Observatory. *Monthly Notices of the Royal Astronomical Society*, 470(3), 2617-2652.

[2] Ahumada, R., Allende Prieto, C., Almeida, A., *et al.* (2020). The 16th Data Release of the Sloan Digital Sky Surveys: First Release of MaNGA Derived Quantities, Data Visualization Tools, and Stellar Library. *The Astrophysical Journal Supplement Series*, 249(1), 3.

[3] Awodey, S. (2010). *Category Theory* (2nd ed.). Oxford University Press.

[4] Baez, J. C., & Dolan, J. (1998). Higher-dimensional algebra and topological quantum field theory. *Journal of Mathematical Physics*, 36(11), 6073-6105.

[5] Cheng, E. (2015). *Cakes, Custard and Category Theory: Easy Recipes for Understanding Complex Maths*. Profile Books.

[6] Cubitt, T. S., Perez-Garcia, D., & Wolf, M. M. (2015). Undecidability of the spectral gap. *Nature*, 528(7581), 207-211.

[7] Forman, R. (1998). Morse theory for cell complexes. *Advances in Mathematics*, 134(1), 90-145.

[8] B. Fornal and B. Grinstein, "Dark Matter Interpretation of the Neutron Decay Anomaly," *Physical Review Letters*, vol. 120, no. 19, p. 191801, 2018.

[9] Gödel, K. (1931). Über formal unentscheidbare Sätze der Principia Mathematica und verwandter Systeme I. *Monatshefte für Mathematik und Physik*, 38(1), 173-198.

[10] Hofstadter, D. R. (1979). *Gödel, Escher, Bach: An Eternal Golden Braid*. Basic Books.

[11] Hou, J., Zhu, G. B., Tinker, J. L., *et al.* (2021). The Completed SDSS-IV extended Baryon Oscillation Spectroscopic Survey: BAO and RSD Measurements from Luminous Red Galaxies in the Final Sample. *Monthly Notices of the Royal Astronomical Society*, 500(1), 1201-1221.

[12] B. Koch and F. Hummel, "An Exciting Hint Towards the Solution of the Neutron Lifetime Puzzle?," *arXiv preprint arXiv:2403.00914*, 2024.

[13] Kitaev, A. (2003). Fault-tolerant quantum computation by anyons. *Annals of Physics*, 303(1), 2-30.

[14] Lawvere, F. W. (1963). Functorial semantics of algebraic theories. *Proceedings of the National Academy of Sciences*, 50(5), 869-872.

[15] Lee, P. C. K. (2024a). Higher Categorical Structures in Gödelian Incompleteness: Towards a Topos-Theoretic Model of Metamathematical Limitations. *viXra.org e-Print archive*, viXra:2407.0164.

[16] Lee, P. C. K. (2024b). The Geometry of Gödelian Categorical Singularities: A Refined Mathematical Framework for Incompleteness Phenomena (Part 2: Extending the Topological and Geometric Aspects). *viXra.org e-Print archive*, viXra:2408.0049.

[17] Lee, P. C. K. (2024c). Ricci Flow Techniques in General Relativity and Quantum Gravity: A Perelman-Inspired Approach to Spacetime Dynamics. *viXra.org e-Print archive*, viXra:2407.0165.

[18] Lee, P. C. K. (2024d). A Ricci Flow-Inspired Model for Cosmic Expansion: New Insights from BAO Measurements. *viXra.org e-Print archive*, https://vixra.org/abs/2408.0067.

[19] Lee, P. C. K. (2024e). Gödelian Index Theorem on Smooth Manifolds: Extending the Atiyah-Singer Framework and Its Cosmological Implications (Part 3 of Categorical Gödelian Incompleteness Series). *viXra.org e-Print archive*, https://vixra.org/abs/2408.0075.

[20] Lee, P. C. K. (2024f). Gödelian Index Theorem in Discrete Manifolds: A Unified Framework for Logical Complexity Across Cosmic and Quantum Scales (Part 4). *viXra.org e-Print archive*, http://viXra.org/abs/2408.0086.

[21] Lurie, J. (2009). *Higher Topos Theory*. Princeton University Press.

[22] Mac Lane, S., & Moerdijk, I. (1992). *Sheaves in Geometry and Logic: A First Introduction to Topos Theory*. Springer-Verlag.

[23] Penrose, R. (1989). *The Emperor's New Mind: Concerning Computers, Minds, and the Laws of Physics*. Oxford University Press.

[24] Ross, A. J., Samushia, L., Howlett, C., *et al.* (2017). The Clustering of the SDSS DR7 Main Galaxy Sample: A 4 per cent Distance Measure at $z = 0.15$. *Monthly Notices of the Royal Astronomical Society*, 464(1), 1168-1184.

[25] Sachdev, S. (2011). *Quantum Phase Transitions* (2nd ed.). Cambridge University Press.

[26] The Univalent Foundations Program. (2013). *Homotopy Type Theory: Univalent Foundations of Mathematics*. Institute for Advanced Study.

[27] Watson, J. D., Onorati, E., & Cubitt, T. S. (2021). Uncomputably complex renormalisation group flows. *arXiv preprint arXiv:2102.05145*.

[28] Wen, X. G. (2004). *Quantum Field Theory of Many-Body Systems: From the Origin of Sound to an Origin of Light and Electrons*. Oxford University Press.

[29] Witten, E. (1989). Quantum field theory and the Jones polynomial. *Communications in Mathematical Physics*, 121(3), 351-399.

[30] Wolfram, S. (2002). *A New Kind of Science*. Wolfram Media.

[31] A. T. Yue et al., "Improved Determination of the Neutron Lifetime," *Physical Review Letters*, vol. 111, no. 22, p. 222501, 2013.